



HAL
open science

Tectonic evolution of Leros Island (Dodecanese, Greece) and correlations between the Aegean Domain and the Menderes Massif

Vincent Roche, Clément Conand, Laurent Jolivet, Romain Augier

► **To cite this version:**

Vincent Roche, Clément Conand, Laurent Jolivet, Romain Augier. Tectonic evolution of Leros Island (Dodecanese, Greece) and correlations between the Aegean Domain and the Menderes Massif. *Journal of the Geological Society*, 2018, 1, pp.836-849. 10.1144/jgs2018-028 . insu-01795049

HAL Id: insu-01795049

<https://insu.hal.science/insu-01795049>

Submitted on 18 May 2018

HAL is a multi-disciplinary open access archive for the deposit and dissemination of scientific research documents, whether they are published or not. The documents may come from teaching and research institutions in France or abroad, or from public or private research centers.

L'archive ouverte pluridisciplinaire **HAL**, est destinée au dépôt et à la diffusion de documents scientifiques de niveau recherche, publiés ou non, émanant des établissements d'enseignement et de recherche français ou étrangers, des laboratoires publics ou privés.

Tectonic evolution of Leros Island (Dodecanese, Greece) and correlations between the Aegean Domain and the Menderes Massif

Vincent Roche^{1,2,3*}, Clément Conand^{1,2,3,4}, Laurent Jolivet⁵ and Romain Augier^{1,2,3}

¹ *Université d'Orléans, Institut des Sciences de la Terre d'Orléans (ISTO), UMR 7327, 45071, Orléans, France*

² *CNRS/INSU, ISTO, UMR 7327, 45071, Orléans, France*

³ *BRGM, ISTO, UMR 7327, BP 36009, 45060, Orléans, France*

⁴ *Laboratoire Géosciences Environnement Toulouse (GET), UMR 5563, 31400, Toulouse, France*

⁵ *Sorbonne Université, CNRS-INSU, Institut des Sciences de la Terre Paris, ITeP UMR 7193, F-75005 Paris, France*

* *Corresponding author (e-mail: rochev26@gmail.com & vincent.roche@cnrs-orleans.fr)*

Abstract: The history of subduction below the Aegean region and Western Anatolia is hampered by a lack of comprehension of the correlations between the Cyclades and the Menderes Massif. The Dodecanese Archipelago, key for this discussion, has received very little attention so far. This study is focused on the island of Leros where two tectono-metamorphic units can be observed; the upper Marina unit and the lower Temenia unit. The field study, including new field mapping and structural observations, reveals that Temenia unit has been exhumed under Marina unit through a top-to-the-NE ductile shearing followed by a top-to-the-SW brittle deformation cutting the Temenia/Marina contact. The description of metamorphic aragonite and blue amphibole, complemented by RSCM thermometry, reveals that Temenia unit has been buried down to at least 20 km along a cold metamorphic gradient. In terms of lithology and paleogeographic affinities, the cover of

Marina unit is similar to the Lycian Nappes that rest on top of the Menderes Massif and belong to the northern margin of the Pelagonian domain. Temenia unit can then be compared to Lower Cycladic Blueschists Nappe, which could in turn be correlated with the cover of the Menderes Massif, which has also recorded a HP-LT metamorphic overprint.

1. Introduction

The effects of the dynamics of subducting slabs (retreat, tearing, detachment etc.) on the tectonic evolution of the overriding plate are still highly debated (Carminati *et al.* 1998; Wortel & Spakman 2000; Piromallo & Morelli 2003; Spakman & Wortel 2004; Faccenna *et al.* 2004, 2005; Govers & Wortel 2005; Jolivet *et al.* 2009, 2013; Sternai *et al.* 2014). The Mediterranean area is certainly the most studied and debated area thanks to the high resolution of seismic tomography data. Under the eastern part of the Aegean Sea and West Turkey all studies suggest a slab tearing well imaged by seismic tomography (Fig. 1) (De Boorder *et al.* 1998; Salaün *et al.* 2012; Biryol *et al.* 2011). Based on the evolution and migration of the magmatic activity and the chronology of paleomagnetic rotations, Jolivet *et al.* (2015) proposed that this slab tearing happened between 20 and 8 Ma with a faster retreat between 15 and 8 Ma coeval with the fast rotation of the Hellenides revealed by paleomagnetic data (Van Hinsbergen *et al.* 2005). Govers & Fichtner (2016) proposed instead that the first tear was formed in the Eocene. Although the age of the tearing is still being discussed, the tectono-metamorphic record in the overriding plate has not yet been fully described, hampering a full comprehension of the coupling between crustal deformation and mantle flow that is suggested by numerical models (e.g. Sternai *et al.* 2014; Menant *et al.* 2016). Ring *et al.* (1999), Gessner *et al.* (2013) and Jolivet *et al.* (2013; 2015) have discussed the existence of a distributed left-lateral shear zone between the Menderes Massif

and the Aegean Sea, accommodating the differential motion of crustal domains above the STEP-fault, but the exact way crustal deformation accommodates this shearing is still unknown. Because of poorly understood correlations between the Aegean Sea and the Menderes Massif, discussing the tectonic evolution of the crust above the tear remains difficult. Between the Menderes Massif and the Aegean domain, the Dodecanese Archipelago (Fig. 1a) has received very little attention so far (e.g. Katagas, 1980; Franz *et al.*, 2005; Ring *et al.* 2017). This paper is focused on one of the largest islands of this Archipelago, Leros, where we have studied the contact between two units belonging to both domains, Aegean and Menderes, in order to precise the geological correlations across the STEP-fault region above the tear.

2. Geological setting

2.1. The Cyclades Archipelago

The Cyclades Archipelago belonging to the Aegean domain is located in the back-arc domain of the Hellenic subduction. This domain has recorded evidence of this subduction-related geodynamics since the Late Cretaceous. Its tectono-metamorphic evolution can be summarized in two major stages: firstly, formation of the Hellenides-Taurides orogenic belt (Late Cretaceous-Eocene; Bonneau & Kienast 1982; Dercourt *et al.* 1986; Van Hinsbergen *et al.* 2005) and secondly post-orogenic extension associated with the retreat of the African slab (Jolivet & Faccenna 2000; Brun & Sokoutis 2010; Jolivet & Brun 2010; Ring *et al.* 2010) accommodated by different crustal-scale detachments such as the North Cycladic Detachment System (NCDS), the West Cycladic Detachment System (WCDS) or the Naxos-Paros Detachment System (Fig. 1a) (Gautier *et al.* 1993; Jolivet *et al.* 2010; Grasemann *et al.* 2012).

In details, the Cyclades Archipelago, west of the Dodecanese, shows a variety of lithologies metamorphosed under blueschist- and eclogite-facies conditions (Blake *et al.* 1981; Bröcker 1990; Okrusch & Bröcker 1990; Jolivet *et al.* 2003, 2004; Brun & Faccenna 2008; Jolivet & Brun 2010; Ring *et al.* 2010) forming the Cycladic Blueschists Unit (CBU), whose formation is linked with the burial and exhumation within a subduction zone during the Eocene and subsequent exhumation during the Aegean Sea formation (Jolivet & Brun 2010, Ring *et al.* 2010). Peak-pressure assemblages spectacularly crop out on the islands of Syros or Sifnos, (e.g. Trotet *et al.* 2001; Groppo *et al.* 2009; Laurent *et al.* 2016; Roche *et al.* 2016) but are also quite well preserved despite retrogression in many other islands (e.g. Avigad *et al.* 1998; Parra *et al.* 2002; Huet *et al.* 2009; Augier *et al.* 2015). There, available P-T estimates point to a common HP-LT event at about 20 – 23 kbar and 550 °C. Recently, Grasmann *et al.* (2018) suggest the existence of two different nappes or subunits within the CBU, the Lower Cycladic Nappe for the lower pressure and the Upper Cycladic Nappe for the higher pressure parageneses. According to this study, these nappes are separated by the newly defined synorogenic Trans Cycladic Thrust (see Fig. 1a, TCT; Grasmann *et al.* 2018). These rocks were mainly exhumed below (1) a syn-orogenic detachment (50 – 35 Ma) cropping out on Syros (Trotet *et al.* 2001; Laurent *et al.* 2016; Roche *et al.* 2016) and (2) post-orogenic detachments (after 35 Ma) such as the NCDS (Jolivet *et al.* 2010), the WCDS (Grasmann *et al.* 2012) or the NPFS (Urai *et al.* 1990; Gautier *et al.* 1993; Bargnesi *et al.* 2013). Most detachments show a top-to-the NE kinematics but the southwest part of the Cyclades shows an opposite top-to-the-SW sense of shear (Grasmann *et al.* 2012). Resting above the CBU and associated detachments, the hanging-wall Pelagonian unit did not go through an episode of subduction during the formation of the Hellenides. Finally, a late high-temperature episode is recorded during the exhumation of Metamorphic Core Complexes (MCCs) in the Middle and Late Miocene with

the formation of migmatite domes in Naxos and Ikaria (Lister *et al.* 1984; Urai *et al.* 1990; Rabillard *et al.* 2015; Beaudoin *et al.* 2015). This stage was accompanied by the emplacement of syn-tectonic Miocene I and S-type granites (i.e. Tinos, Mykonos, Ikaria, Naxos, Serifos or even Lavrio) (Jansen 1973; Lee & Lister 1992; Altherr & Siebel 2002; Grasemann & Petrakakis 2007; Iglseder *et al.* 2009; Rabillard *et al.* 2015).

2.2. The southwestern part of Turkey

The southwestern domain of Turkey is composed of several tectonic units. The Menderes Massif is mainly made up of basement units stacked during the Eocene (e.g. Ring *et al.* 2010; Gessner *et al.* 2001; Bozkurt & Oberhänsli 2001; Bozkurt 2001; Cenko-Tok *et al.* 2016). The core of the massif mainly shows a high-temperature overprint while the Permian-Mesozoic cover visible in the south has recorded HP-LT conditions (10 – 12 kbar and 440 °C) (Rimmelé *et al.* 2003). Immediately above, the Lycian Nappes, composed of a Permian-Triassic complex and Jurassic-Cretaceous marbles, overlain by the Menderes cover (Rimmelé *et al.* 2005) and HP-LT metamorphic assemblages (8 – 10 kbar and 420 °C) are observed in the basal unit (Karaova unit or Ören unit) (Rimmelé *et al.* 2003; Pourteau *et al.* 2013). A third unit, the CBU, locally occurs between the Menderes Massif and the Lycian Nappes. On its northern and eastern margins, the Menderes Massif is overthrust by the Afyon Zone and the Tavşanlı Zone, both with HP-LT parageneses. Both units are overthrust by the oceanic units of the Izmir-Ankara Tethyan suture zone. The Lycian Nappes root within the suture zone, as shown by the presence of klippe of HP-LT metamorphics with Fe-Mg carpholite on top of the Menderes Massif. The Menderes basement is affected by several Miocene low-angle detachments, later cut by steeply-dipping normal faults controlling the major Simav, Gediz-Alaşehir and Büyük Menderes active

grabens. In the north, extension is associated with the formation of migmatites in the Early Miocene (Cenki-Tok *et al.* 2016). The direction of extension is NNE-SSW and bivergent (Gessner *et al.* 2013). Along the upper contact of the Menderes Massif, E-W and NE-SW stretching lineations and top-to-the-E/NE kinematics are documented within the basal unit of the Lycian Nappes (Ören unit or Karaova unit, see Rimmelé *et al.* 2006 and Pourteau *et al.* 2013) suggesting the presence of a top-to-the-E/NE detachment between the Menderes Massif and the Lycian Nappes during the earlier exhumation of HP-LT rocks (Rimmelé *et al.* 2003).

2.3. The Dodecanese Archipelago

The Dodecanese Archipelago is mostly composed of metamorphic rocks belonging to different units that experienced very different P-T evolutions, from MT-MP conditions (i.e. upper greenschist to lower amphibolite-facies conditions) of probable Late Paleozoic age (Franz *et al.* 2005) to HP-LT conditions probably coeval with the Eocene subduction history of the Cyclades on Leros, Kalymnos, Lipsi (Franz *et al.* 2005) or on Arki (Franz & Okrusch 1992). These rocks are unconformably covered with shallow marine sediments of probable Miocene age (Stavropoulos & Gerolymatos 1999). More recent magmatic rocks are observed on Patmos and Kos (Wyers & Barton 1986).

Very few studies were published on the geology of Leros Island. Katagas and Sapountzis (1977) distinguished four tectono-metamorphic units, which Franz *et al.* (2005) then grouped in only two, Temenia and Marina units, covered with a sedimentary unit attributed to the Miocene. Marina unit, further divided into two subunits, Panormos and Emporios (Franz *et al.* 2005), is composed of amphibolites and garnet-micaschists (pre-

Alpidic basement) and a poorly metamorphosed sedimentary cover composed of Permo-Triassic metapelites (i.e. siliciclastic Verrucano metasediments), metasandstones and Jurassic marbles (i.e. well bedded metacarbonate rocks; Fig. 2). The pre-Alpidic basement of this unit had recorded two metamorphic episodes, a first Variscan (320 – 300 Ma K/Ar on amphiboles and white micas) characterized by high-temperature and low-pressure (MT-MP) conditions and a second one associated with the Alpine orogeny, displaying greenschist-facies metamorphic parageneses. Based on a petrological study and on the chemical composition of garnets from garnet-micaschists of Marina unit, Franz *et al.* (2005) proposed P-T conditions up to 570 – 630 °C and 6 – 8 kbar for the Variscan episode and a very weak overprint at around 300 – 350 °C at ca. 2 – 3 kbar for the Alpine episode. Temenia unit structurally underlies Marina unit through a shallow-dipping tectonic contact. It is mainly composed of schists, intercalated marble layers and rare occurrences of metabasites where HP-LT parageneses are preserved. Temenia unit also includes a thick marble layer that shapes the landscape in the southeastern part of the island. This unit has undergone an Alpine HP-LT metamorphism (Katagas & Sapountzis 1977; Franz & Okrusch 1992) with a peak-thermal conditions of 300 – 400 °C at 7 kbar. In most cases the basement of Marina unit rests on top of Temenia through a shallow-dipping contact, but the cover of Marina unit is in places in direct contact with Temenia unit with no intervening basement. Otherwise, the non-metamorphic sediments (clastics and carbonates) attributed to the Miocene, rest on top of all metamorphic units. The HP-LT metamorphic parageneses of the lower unit (Temenia) and the metamorphic gap between Marina and Temenia units raise the question of potential detachments similar to the Cycladic ones, below Miocene sediments or between Temenia and Marina units.

3. A new structural map of Leros

The field survey and the satellite image analysis performed during this study allow us proposing a new geological map of Leros that complements the geologic map of Stavropoulos and Gerolymatos (1999). Results are shown in Figures 2 and 3. Besides, this study brings the first tectonic map of the island including the recognition of the large-scale geometries, main structures and kinematics of deformation whether ductile or brittle. This map also indicates stretching lineations and kinematic indicators, as well as the nature of contacts and their kinematics. A tectono-stratigraphic log presents the three different units Temenia, Marina and Miocene sediments and three cross-sections complete the description of the geometrical relations between units and their deformation (Figs. 3).

4. Kinematics of deformation

4.1. Ductile deformation

The ductile deformation recorded in both Marina and Temenia units shows clear gradients when approaching the main contact zones identified during field mapping. Foliation and stretching lineations were systematically measured all over the island and kinematic indicators noted when present (Fig. 4). More than 680 foliations were measured over the island in all lithologies. In average, the foliation strikes N150°E and dips about 30° toward the ENE in both units, but also shows a significant dispersion because of intense folding, as well as boudinage (Fig. 3). For instance, the first cross-section (Fig. 3a) indicates highly variable thickness of the pre-Alpidic basement and, more locally the lack of Permian-Triassic metasediments. Large-scale boudinage of marbles in the southeast of the island,

obvious in the landscape confirms also the kilometric-scale of boudinage of Temenia unit (Fig. 5a). In addition, this unit shows large variations in folding style and intensity with localization of folding in specific areas. The distribution of foliation poles at the scale of Temenia unit (Fig. 2) suggests that fold axes are trending N40°E in average and dip 30° toward the NE.

Stretching lineations are marked by various types of indicators, depending upon the lithology, intensity of the deformation and P-T conditions: elongation of quartz and mica aggregates in metapelites (Temenia and Marina basement), of epidote and blue-amphiboles in HP metabasites (Temenia), hornblende in amphibolites (Marina basement) and stretched clasts in meta-conglomerates (Permo-Triassic). On most outcrops, the orientation of various types of lineation is constant. However, the strike of lineations shows a quite large dispersion, trending between N°0 and N°90 (Fig. 3a). It is centered on an average NE direction (Fig. 3a), with variable NE plunges in both Marina and Temenia units.

Besides systematic measurements of stretching direction, the sense of shear has been studied. Although rocks are generally pervasively deformed, reliable kinematics indicators are not very common and quite unequally distributed over the Island. In addition, we focus mainly on the study of the deformation within Temenia unit (Figs. 3a and 4), which presents HP-LT Alpine parageneses. Most monoclinic structures are visible in the northern part of Temenia unit close to the contact with Marina unit. Shear bands with a consistent dip deflect the foliation (Fig. 4a) and the most competent levels are also sheared and affected by quartz veins perpendicular to the stretching direction. These structures are present at the centimetre scale (Fig. 4a) but also pluri-metric (Figs. 4b and 4c), illustrating the penetrativity of deformation. The sense of shear indicated by shear bands is top-to-the-

north or top-to-the-northeast, reflecting the sense of motion along the contact between Marina and Temenia units. Opposite shear sense can be locally observed, especially near Agios Isidoros (Fig. 2), where the observed shearing deformation is mostly accommodated by localized shear bands associated with veins evolving toward cataclasites, not by an intense penetrative deformation, suggesting conditions close to the brittle-ductile transition in these alternations of marbles and metapelites close to the contact.

The basement of Marina unit has undergone a strong ductile deformation but shows no systematic kinematic indicators. Part of the basement has been intensely deformed under Barrovian metamorphic conditions leading to the development of a foliation and stretching lineation in amphibolites and garnet-bearing micaschists, but this deformation, closely associated with the MT-MP metamorphic conditions is related to a pre-Alpine event. On the opposite, the Mesozoic marbles of Marina unit display an intense boudinage visible at all scales, from the centimetre to several hundreds of meters leading to large thickness variations of the Permo-Triassic formation (Fig. 3). Further north, Figure 5b shows the boudinaged cover of Marina resting both on Temenia unit and on the basement of Marina unit showing that boudinage has locally totally eliminated Marina basement.

4.2. Brittle deformation

Although large-scale brittle structures are quite rare, the whole island of Leros is pervasively affected by brittle deformation (e.g. Fig. 6) that post-dates ductile features. In the western part of the island (Fig. 2), the geometrical relations between the Neogene sediments and the metamorphic units can be observed. A second deformation stage, with a

top-to-the-SW kinematic, and mostly brittle, is recognized along the main contact in three main areas of the island. The first is in the area of the island of Agios Isidoros (Fig. 6a), where the ductile deformation within Temenia is very intense and becomes more brittle approaching the base of Marina unit with SW-dipping shear bands and faults. In addition, the contact between Temenia and Marina marbles in the village of Xirokampos (Fig. 2) is also faulted with a steeper dip and a top-to-the-SW kinematics (Fig. 6b). Finally, the same kinematics is observed west of Lakki (Fig. 3), where a low-angle fault plane is observed along the contact between Neogene sediments and metamorphic units (Fig. 6c).

There, sediments west of Lakki display a rollover geometry with a fan thickening toward the low-angle west-dipping normal fault (Fig. 6d), showing the syn-extensional history of these deposits. These sediments, at their eastern limit, are in fault contact with a marble lens of Marina cover (Fig. 6e) but also with Temenia schists and marbles alternation. Below the low-angle normal fault, the marbles of Marina unit are highly faulted and brecciated across a few tens of meters (Fig. 6f). Normal faults within the breccia are generally more steeply dipping than the main fault plane, but the direction of stretching deduced from the striated fault set is compatible with the same direction of extension. All faults, small and large ones, steep or low-angle, are normal. They strike in average N130°E and dip between 10 and 70° toward the SW. The main fault shows the superimposition of two sets of striation (Fig. 6g), the first one trending N50°E and the second one N130°E. The lower contact between the marble lens and Temenia schists is also faulted, with the same orientation as the sediment/marble contact. The first set of striation along the main plane and on smaller scale faults in the breccia is compatible with a NE-SW extension (N31°E in average) compatible with the normal throw on the main contact and with the syn-

deposition tilt of the Neogene sediments. The second set of striation indicates a more N-S direction of extension (167°N in average) showing a late reactivation of the fault, still at shallow dip. In the northwest of Leros, the Neogene sediments rest with a depositional contact on the Permo-Triassic sandstones and microconglomerates and are cut by late normal faults.

The observed Alpine structures within metamorphic units and at their contact with the Neogene sediments thus show a continuum of NE-SW stretching from ductile to brittle conditions. It starts with boudinage of all units, especially Marina that is locally partly eliminated and continues with top-to-the-NE shearing deformation within Temenia unit with a focalization along the contact between the two units. Locally, the sense of shear is opposite showing that a significant component of co-axial flow should be taken into account. The same stretching direction is observed in the first stages of brittle deformation along the contact with the sediments that are deposited during the activity of the shallow west-dipping normal fault west of Lakki. This continuum of deformation from ductile to brittle suggests that the early ductile deformation is also due to an extensional event. A late extensional event has reactivated the shallow-dipping normal fault with a more northerly direction of stretching.

5. Metamorphic record and P-T estimates in metamorphic units

The metamorphic record was investigated throughout Leros Island. Because most of the Island is composed by accreted sediments lacking metamorphic index minerals, except for amphibolites and garnet micaschists of the Marina unit that experienced a pre-Alpine

Barrovian metamorphic event, constraints on the Alpine HP-LT metamorphic conditions remain very sparse. In a first attempt to describe the metamorphic architecture of Leros and to put constraints on the metamorphic evolution of each unit, we performed a detailed analysis of the parageneses carried by different types of lithologies present on Leros. By contrast, rocks of Leros are often rich in carbonaceous material (CM) and are therefore particularly appropriate for RSCM (Raman Spectroscopy of CM) thermometry. Results are all presented in Figure 7 and some representative field examples are given in Figure 8.

5.1. Conventional metamorphic petrology observations

Rocks exposed on Leros show rather high variance mineral assemblages either for metacarbonate rocks or even metapelites. Parageneses in metabasites, which are a straightforward field indicator of P-T conditions, were particularly studied in the different units. This analysis was refined and strengthened by the recognition of index-minerals in other lithologies.

At a first glance, two different types of conditions are clearly recorded in Marina unit. The basement rocks of Marina unit recorded Barrovian MT-MP conditions while the cover series escaped significant Alpine imprint. In the basement, massive metabasite and micaschist are the best candidates to study metamorphic parageneses. There, hornblende and plagioclase (amphibolite facies metabasites) and garnets, muscovite and quartz (metapelites) are very common and well preserved (Figs. 8a and 8b). Rocks from the cover series do not provide any reliable markers of the metamorphic grade although deformation was recorded in the ductile regime. Metacarbonate rocks show calcite recrystallization and the rare intercalations of metapelites show only the growth of phyllosilicates. In the

southern part of the island, the marbles of Temenia unit locally contain a dark carbonate mineral, with a fibrous and radiating structure suggesting the presence of aragonite (Figs. 7, 8c) that was validated by Raman spectroscopy (Fig. 8d). In this unit, foliation in metabasites is mainly defined by blue amphibole needles quartz and epidote. Blue amphiboles (Appendix, Table 1) show strong pleochroism without clear inclusions. Relic of crenulation cleavage marked by blue amphiboles are locally observed whereas others defined the main foliation (Fig. 8e). They show a quite strong chemical zoning (Fig. 8e), with a chemical core composition range from glaucophane/crossite (Na-amphiboles) to winchite (Na-Ca amphiboles) (Fig. 8e). According to the IMA nomenclature (e.g. Leake *et al.*, 1997), the rim of blue amphiboles are ferriwinchites (Fig. 8f). Metamorphic assemblages present in metabasites therefore show HP-LT metamorphic conditions where the mineral assemblage recognized in the blueschists is glaucophane/crossite - chlorite - phengite - epidote - quartz \pm albite \pm hematite \pm rutile \pm titanite, conforming to the epidote-blueschist facies of Evans (1990). This assemblage is variably overprinted into greenschist-facies conditions in which blue amphibole breaks down to chlorite. The conventional ACF diagram would indicate a cross reaction as follows: epidote + glaucophane + quartz \rightleftharpoons winchite + chlorite + albite. The associated greenschist-facies thus display the following paragenesis chlorite - phengite - epidote - albite - quartz - winchite - calcite - rutile. The only white micas recorded in the blueschists rocks are phengites (Fig. 8g; Appendix, Table 2) with high silica content (3.30 – 3.60 Si p.f.; Fig. 8g). Epidote and chlorite ($X_{Mg} \approx 0.72$; Appendix, Tables 3 and 4) also have relatively homogeneous compositions. Even if our chlorite compositions are richer in magnesium than the ones described in Franz & Okrusch (1992) in blueschists from the Temenia unit of the nearby island of Arki, other mineral (i.e. epidote, phengite and blue-amphibole) show very similar compositions.

5.2. RSCM thermometry

Raman spectroscopy on carbonaceous material (RSCM) allows determining the maximum temperature experienced by the rock sample (Beyssac *et al.* 2002). The technique is based upon the observation that sedimentary carbonaceous material (CM) is progressively transformed into graphite with increasing metamorphism (Pasteris & Wopenka 1991; Wopenka & Pasteris 1993). The degree of organization of the CM is quantitatively characterized by Raman spectroscopy and because of the irreversible character of graphitization, CM structure only depends on the maximum T (T_{\max}) reached during metamorphism, regardless of the shape of the retrograde path during exhumation (Beyssac *et al.* 2002). T_{\max} can be determined in the range 330 – 650 °C with an accuracy of ± 50 °C due to uncertainties on petrologic data used to calibrate the thermometer. Relative uncertainties on T attached to a series of samples are however as low as 10 – 15 °C (e.g. Beyssac *et al.* 2004; Brovarone *et al.* 2013).

Raman spectra were obtained using the Renishaw InVia Reflex system (BRGM-ISTO, Orléans). RSCM analyses were conducted on thin sections prepared on CM-rich metasediments (metapelites and marbles) cut in the structural (i.e. X-Z, plane orthogonal to foliation and parallel to lineation). To avoid defects on the CM related to thin-section preparation, analyses were all performed below the surface of the section by focusing the laser beam beneath a transparent crystal such as quartz and calcite. Spectra were all obtained and then treated using Peakfit software following the procedure described in Beyssac *et al.* (2002).

To document the Peak-T conditions and the distribution of the Alpine metamorphic event, this thermometric study primarily focuses on Temenia unit. Samples from Marina unit (basement and cover) were also studied in order to compare the thermal evolution of the two units and the T_{\max} values with P-T estimates previously published (Franz *et al.* 2005). However, since this method provides the maximum temperature ever experienced reached by the rock, it is impossible to obtain the conditions for a potential Alpine overprinting on Marina basement during subduction, because the temperature would not exceed the Variscan peak (570 – 630 °C) estimated by Franz *et al.* (2005).

RSCM results are all plotted on a map (Fig. 7) and projected on the different cross-sections to locate them in the units and relative to tectonic contacts (Fig. 3b). Detailed results, including R2 ratio, number of spectra, T_{\max} and standard deviation are presented in Table 1. 13 – 22 spectra were routinely recorded for each sample to smooth out the inner structural heterogeneity of CM within samples that is generally low.

Metasediments of Leros show significant variations in the structural organization of CM and then significant temperature variations (Table 1) from one unit to another. Temperatures range from ca. 350 °C of the cover series and up to 600 °C deduced from Marina basement rocks. As a general overview, Temenia unit yielded spectra exhibiting decreasing D1 and D2 defect bands relatively to the G graphite band compared to the cover of the Marina unit (e.g. Beyssac *et al.* 2003). Such evolution can be interpreted as due to a general T decrease of one hundred degrees (e.g. Beyssac *et al.* 2002). In details, temperatures deduced from Marina cover yielded very consistent results in the narrow range of 349 ± 6 and 387 ± 27 °C. A garnet micaschist sample of Marina basement (sample 16-302) yielded a temperature of 602 ± 18 °C. This temperature falls in the range 570 – 630 °C estimated by Franz *et al.* (2005) for the peak-temperature conditions attributed to a former Variscan event.

It appears therefore possible to constrain peak-temperature conditions for the Alpine events for all cover series of the Marina unit. Conversely, the intensity of Alpine events can not be constrained into the basement rocks due to the Variscan metamorphic imprint. In Temenia unit, T_{\max} values obtained in the dark marbles and micaschists fall in the range between 368 ± 11 °C and 487 ± 17 °C. The results obtained in other lithologies show a quite constant T_{\max} (Fig. 7). In addition, aragonite marbles, located in the southern part of the island (Fig. 7), were also studied with the RSCM method to estimate T_{\max} . They yielded a temperature of 368 ± 11 °C whereas the upper structural levels give a T_{\max} around 439 °C in schist reaching 387 °C in the marbles (Fig. 7).

6. Discussion

6.1. Structural and metamorphic evolution

The two main units recognized on Leros, Marina and Temenia, are superimposed through a low-angle tectonic contact. The most visible ductile deformation is associated with NE-SW stretching and a majority of top-to-the-north or -northeast kinematic indicators but, locally, even along the main contact, the opposite sense of shear can be observed (Fig. 4d), especially during the latest increments of deformation across the brittle-ductile transition (Fig. 6a). Almost all of these ductile shear criteria are observed in Temenia unit, close to the contact with the cover of Marina unit. In these areas, the Permo-Triassic sediments are often absent or highly thinned down to a few meters and intensely deformed, while they can reach several tens of meters elsewhere. No significant deformation is instead observed at the contact between the basement and the cover of Marina unit indicating no reactivation of this original unconformity.

A significant gap of temperature of ~ 100 °C is observed between Marina and Temenia units showing that some crustal thickness is missing across the contact, suggesting that it acted as an extensional detachment. A second-order tectonic contact between the upper marbles of Temenia containing aragonite and the lower part of the unit also shows a gap in T_{\max} , further suggesting that the thinning of the nappe pile was accommodated by several yet minor shear zones. Using the RSCM T_{\max} constraints together with the constraint of the occurrence of aragonite, this sample must have attained at least 8 kbar, assuming that the peak of pressure was coeval with the peak of temperature (~ 368 °C, Fig. 9). The maximum pressure is also constrained by the presence of the celadonite-rich phengite, epidote and Na-amphiboles. According to Evans (1990), the P-T field of the epidote-blueschist-facies strongly depends on the composition of the Na-amphiboles. The Na-amphiboles of Leros range from glaucophane to crossite equivalent to Evans' grids #5 and #6. The resulting P-T range experienced by the rocks of Leros is strongly reduced by the stable occurrence of albite and aragonite and by the RSCM T_{\max} temperatures for these both samples implying therefore a cold HP-LT gradient (Fig. 9). Temenia unit was thus subducted down to at least 20 km along a HP-LT gradient compatible with an active subduction context and later exhumed and thinned below a shallow-dipping tectonic contact with a top-to-the-NE kinematics.

Furthermore, the large-scale structure reveals a boudinage of the basement of Marina unit that is locally missing between the cover and Temenia unit. Temenia marbles also show large-scale boudinage visible in the landscape. Although most of kinematic indicators are top-to-the-NE, this boudinage and the late brittle deformation shows a significant component of coaxial flow in the deformation history of both Temenia and Marina units

with a progressive localization along the main contact. In the latest stage, low-angle west-dipping normal faults controlled the deposition of shallow-marine Neogene sediments. The exhumation history is in good agreement with the average direction of stretching accommodated by the main Aegean detachments during the Oligo-Miocene (Jolivet *et al.* 2010; Grasemann *et al.* 2012).

6.2. Large-scale correlations

The two tectonic units of Leros Island have recorded drastically different metamorphic histories, Marina unit having escaped a deep burial in a subduction zone and conversely preserve a strong Variscan imprint. Temenia unit instead carries unambiguous evidences of subduction but with maximum P-T conditions far less severe than the typical CBU that show higher-pressure blueschists and eclogitic conditions reaching 550 °C and 22 kbar on Syros, Sifnos or even Sikinos (e.g. Trotet *et al.* 2001; Groppo *et al.* 2009; Augier *et al.* 2015). On Leros, P-T-conditions of the epidote-blueschist-facies did not exceed 450 °C and are quite consistent to conditions deduced by Franz & Okrusch (1992) in comparable blueschists from the Temenia unit of Arki island. These conditions are also similar to some of the more external CBU such as those observed on Folegandros for instance (Augier *et al.* 2015) or Milos where metamorphic conditions are at 8.5 ± 2.0 kbar (Fig. 9) (Grasemann *et al.* 2018). These rocks were thus buried along a common cold P-T gradient along the subduction zone but escaped the much higher conditions experienced in the subduction channel on Syros or Sifnos.

In terms of lithologies, Temenia unit shows a mixture of metapelites and marbles with minor metabasite occurrences that can also be correlated with the metamorphic sequence of Folegandros (Augier *et al.* 2015). Although there is a lack of massive metabasite bodies compared to the “classical” CBU, the metamorphic sequence may however represent a regional lithological variation of the same paleogeographic domain, subducted to shallower depths. It is thus possible to correlate Temenia unit with the Lower Cycladic Nappe described by Grasemann *et al.* (2018) that encompasses tectonic units belonging to the CBU but with lower maximum pressure (i.e. 8 – 9 kbar) than the Upper Cycladic Nappe that have recorded eclogite-facies conditions. As the Upper Cycladic Nappe is also a terminology used for the uppermost unit of the Cyclades belonging to the Pelagonian domain (devoid of any Eocene HP-LT overprint) (e.g. Reinecke *et al.* 1982), we prefer, in order to avoid possible confusion, to use for these two units the “Lower Cycladic Blueschists Nappe” for the lower pressure parts and the “Upper Cycladic Blueschists Nappe” for the higher pressure ones (Fig. 1a).

An alternative correlation of Temenia unit is with Ören unit, the lower metamorphic part of the Lycian Nappes. Peak metamorphic conditions in Ören unit are estimated at 8 kbar and 420 °C, thanks to the presence of Fe-Mg carpholite in the dark micaschists, aragonite in marbles and blue amphiboles in the overlying flysch (Rimmele *et al.* 2003). The sedimentary sequence of Leros is however quite different from the Ören unit that shows a more developed Permo-Triassic reddish and purple sequence and more typical metapelites with dark micaschists where Fe-Mg carpholite is present in large amounts.

Furthermore, a possible correlation with the Phyllite-Quartzite Nappe (PQN) of Crete could be envisaged. However the PQN shows ubiquitous HP-LT parageneses, characterized

by the presence of Fe-Mg carpholite with maximum pressure above 16 kbar (Seidel *et al.* 1982; Theye *et al.* 1992; Jolivet *et al.* 1996; Jolivet *et al.* 2010), which is at odd with our observations on Leros. Then, the PQN is also composed of a thick pile of metapelites and meta-sandstones with minor carbonates, which makes an important additional difference with Temenia unit.

On Leros, the low-grade metamorphic Lycian Marina unit rests on top of the Lower Cycladic Blueschists Nappe. Although the metamorphic grade changes toward Western Turkey, superposition of the same broad paleogeographic units is observed with the Lycian Nappes (i.e. small klippen of the Ören unit) on top of the CBU (Oberhänsli *et al.* 1998; Rimmelé *et al.* 2006). This unit may be thus correlated with a less metamorphosed lateral equivalent of the Lycian Nappes. One major difference between Marina unit cropping out on Leros and the Lycian Nappes is however the presence of a pre-Alpine basement always lacking in Turkey. If we accept this paleogeographic correlation with the Lycian Nappes, the origin of this basement should be looked for in the root zone of the Lycian Nappes, north of the Menderes Massif or the Afyon Zone (Fig. 1a). Although the contact now observed has been strongly reactivated during exhumation and post-orogenic extension, there is no doubt that it was indeed originally a thrust as the Paleozoic basement of Marina unit rests on top of the Mesozoic Temenia metasediments. The difference in maximum pressure across this contact however calls for large displacements responsible for the omission of at least 10 – 15 km of the original thickness of the accretionary wedge. In addition, the Lycian Nappes are in a structural position at the top of the tectonic pile similar to that of the Pelagonian domain in the Cyclades (i.e. the so-called Upper Cycladic Nappe).

Furthermore, this proposed correlation raises the question of the relationships between the Lower Cycladic Blueschists Nappe and the Menderes Massif: can a lateral equivalent be observed in Western Turkey? In terms of metamorphic grade, the Kurudere Unit, resting on top of the Menderes Massif in the south (Rimmelé *et al.* 2005), between the Menderes basement and the Lycian, has been interpreted as a lateral equivalent of the CBU (e.g. Ring *et al.* 1999; Pourteau *et al.* 2015). In that case, it would rather correspond to the Lower Cycladic Blueschists Nappe where the metamorphic grade is lower and garnet absent, and therefore not to the Upper Cycladic Blueschists Nappe. It would thus be a different unit from the CBU found on Dilek Peninsula that has recorded higher P-T conditions.

To sum-up, these correlations of Leros tectonic units show that the Cycladic HP-LT nappe stack can probably be extended toward the Dodecanese Archipelago and even the Menderes Massif (Fig. 1). Like in Western Turkey, the Lycian Marina unit rests through an original thrust contact on top of the Temenia unit. The relations between these two tectonic units should thus be studied.

6.3. Tectonic implications in the Eastern Aegean domain

Like in most of the Aegean Sea, this part of the CBU was exhumed below a long-angle detachment with a NE-SW direction of stretching and a predominant top-to-the NE kinematics. These kinematics of deformation during exhumation recorded on Leros can be attributed to two possible events. It can either be the same exhumation and extension as in the Cyclades, NE-SW oriented and mostly top-to-the-NE, accommodated first during syn-

orogenic exhumation and then during back-arc extension (e.g. Jolivet *et al.* 2010), or an earlier event, coeval with the exhumation of the metamorphic part of the Lycian Nappes (i.e. the Ören unit) that is in average more E-W than the Aegean extension (Fig. 1a). The observation of a continuum of NE-SW extension on Leros which ends in the brittle field controlling the deposition of Neogene sediments is in favour of the first hypothesis.

The main direction of stretching within Temenia unit is thus related to its exhumation and clusters around NE-SW with a predominant shear sense toward the NE. This is an echo of the Aegean Oligo-Miocene back-arc extension with a progressive evolution toward more brittle conditions. One can thus notice that the main direction of extension on Leros is not significantly different from that of the Cyclades and the Menderes. This shows that the gradient of retreat between the Menderes Massif and the Cyclades, accommodated through a wide shear zone (Gessner *et al.* 2013; Jolivet *et al.* 2015) does not lead to a complex kinematic pattern in the crust of the overriding plate, further suggesting that the flow of mantle underneath, within the tear, is simple, as suggested by the seismic anisotropy pattern below this region (Jolivet *et al.* 2009).

7. Conclusion

This first study of the tectono-metamorphic evolution of Leros Island in the Dodecanese Archipelago fills a gap in the knowledge of the Aegean region. Rough estimates on the P-T conditions in Temenia unit call for a subduction-type gradient with HP-LT conditions and a pressure around 8 – 10 kbar for a temperature ranging from 370 °C to 450 °C, whereas Marina unit does not show any strong Alpine HP-LT overprint. The main

deformation observed on Leros is related to the exhumation of both units with a preferential localization of strain along their contact with a top-to-the NE sense of shear and a large component of coaxial shear. A ca. 100 °C gap is recorded between the two units showing that the contact removed some 10 km or more of the initial thickness of the accretionary wedge. This study shows the superposition of Marina unit, correlated with the Lycian Nappes, on top of Temenia unit, a probably equivalent of the Lower Cycladic Blueschists Nappe in terms of metamorphic conditions and lithologies. This superposition of the Lycian Nappes on the CBU has already been observed in the Menderes Massif. However, a possible correlation of Temenia unit with the cover of the Menderes Massif cannot be ignored and needs to be tested by further research. Leros thus makes a link between the Cyclades and the Menderes Massif in terms of correlation of units and in terms of deformation during exhumation. With some lateral differences, the main units are found on either side of the coastline with the same vertical arrangement and some differences in the grade of metamorphism. In order to reinforce these conclusions, this study should be extended toward the north where the Dodecanese and Eastern Aegean islands of Lipsi, Arki and Fourni that have also received very little attention so far. This would also complete the kinematic pattern during back-arc extension above the slab tear and allow discussing the relations between crustal deformation and mantle flow above the tear.

This work has received funding from the Labex Voltaire homed at Orléans University and BRGM, from the European Research Council (ERC) under the seventh Framework Programme of the European Union (ERC Advanced Grant, grant agreement No 290864, RHEOLITH), and from the Institut Universitaire de France. The authors are grateful to A. Lahfid (BRGM) for assistance during the RSCM session to find the aragonite, to I. Di Carlo (ISTO) for assistance during the numerous electron microprobe sessions, and to S. Janiec

and J.G. Badin (ISTO) for the preparation of thin sections. The paper benefited from relevant revisions by Bernhard Grasemann and Leander Franz.

References

- Altherr, R., & Siebel, W. 2002. I-type plutonism in a continental back-arc setting: Miocene granitoids and monzonites from the central Aegean Sea, Greece. *Contributions to Mineralogy and Petrology*, 143(4), 397-415.
- Augier, R., Jolivet, L., Gadenne, L., Lahfid, A., & Driussi, O. 2015. Exhumation kinematics of the Cycladic Blueschists unit and back-arc extension, insight from the Southern Cyclades (Sikinos and Folegandros Islands, Greece). *Tectonics*, 34(1), 152–185. <https://doi.org/10.1002/2014TC003664>
- Avigad, D., Baer, G., & Heimann, A. 1998. Block rotations and continental extension in the central Aegean Sea: palaeomagnetic and structural evidence from Tinos and Mykonos (Cyclades, Greece). *Earth and Planetary Science Letters*, 157(1), 23-40.
- Bargnesi, E. A., Stockli, D. F., Mancktelow, N., & Soukis, K. 2013. Miocene core complex development and coeval supradetachment basin evolution of Paros, Greece, insights from (U-Th)/He thermochronometry. *Tectonophysics*, 595–596, 165–182. <https://doi.org/10.1016/j.tecto.2012.07.015>
- Beaudoin, A., Augier, R., Laurent, V., Jolivet, L., Lahfid, A., Bosse, V., ... Menant, A. 2015. The Ikaria high-temperature Metamorphic Core Complex (Cyclades, Greece): Geometry, kinematics and thermal structure. *Journal of Geodynamics*, 92, 18–41. <https://doi.org/10.1016/j.jog.2015.09.004>
- Beysac, O., Goffé, B., Chopin, C., & Rouzaud, J. N. 2002. Raman spectra of carbonaceous material in metasediments: A new geothermometer. *Journal of Metamorphic Geology*, 20(9), 859–871. <https://doi.org/10.1046/j.1525-1314.2002.00408.x>
- Beysac, O., Brunet, F., Petit, J. P., Goffé, B., & Rouzaud, J.-N. 2003. Experimental study of the microtextural and structural transformations of carbonaceous materials under pressure and temperature, *Eur. J. Mineral.*, 15, 937–951.
- Beysac, O., Bollinger, L., Avouac, J. P., & Goffé, B. 2004. Thermal metamorphism in the lesser Himalaya of Nepal determined from Raman spectroscopy of carbonaceous material. *Earth and Planetary Science Letters*, 225(1), 233-241.
- Biryol, C., Beck, S. L., Zandt, G., & Özacar, A. A. 2011. Segmented African lithosphere beneath the Anatolian region inferred from teleseismic P-wave tomography.

- Geophysical Journal International*, 184(3), 1037–1057. <https://doi.org/10.1111/j.1365-246X.2010.04910.x>
- Blake, M. C., Bonneau, M., Geyssant, J., Keinast, J. R., Lepvrier, C., Maluski, H., & Papanikolaou, D. 1981. A geologic reconnaissance of the Cycladic blueschist belt, Greece. *Geological Society of America Bulletin*, 92(5), 247. [https://doi.org/10.1130/0016-7606\(1981\)92<247:AGROTC>2.0.CO;2](https://doi.org/10.1130/0016-7606(1981)92<247:AGROTC>2.0.CO;2)
- Bonneau, M., & Kienast, J. R. 1982. Subduction, collision et schistes bleus; l'exemple de l'Egee (Grece). *Bulletin de La Société Géologique de France*, S7–XXIV(4), 785–791. <https://doi.org/10.2113/gssgfbull.S7-XXIV.4.785>
- Bozkurt, E. 2001. Neotectonics of Turkey – a synthesis. *Geodinamica Acta*, 14(1–3), 3–30. [https://doi.org/10.1016/S0985-3111\(01\)01066-X](https://doi.org/10.1016/S0985-3111(01)01066-X)
- Bozkurt, E., & Oberhänsli, R. 2001. Menderes Massif (Western Turkey): Structural, metamorphic and magmatic evolution - A synthesis. *International Journal of Earth Sciences*, 89(4), 679–708. <https://doi.org/10.1007/s005310000173>
- Bröcker, M. 1990. Blueschist-to-greenschist transition in metabasites from Tinos Island, Cyclades, Greece: Compositional control or fluid infiltration? *Lithos*, 25(1–3), 25–39. [https://doi.org/10.1016/0024-4937\(90\)90004-K](https://doi.org/10.1016/0024-4937(90)90004-K)
- Brovarone, A. V., Beyssac, O., Malavieille, J., Molli, G., Beltrando, M., & Compagnoni, R. 2013. Stacking and metamorphism of continuous segments of subducted lithosphere in a high-pressure wedge: the example of Alpine Corsica (France). *Earth-Science Reviews*, 116, 35–56.
- Brun, J. P., & Faccenna, C. 2008. Exhumation of high-pressure rocks driven by slab rollback. *Earth and Planetary Science Letters*, 272(1–2), 1–7. <https://doi.org/10.1016/j.epsl.2008.02.038>
- Brun, J.-P., & Sokoutis, D. 2010. 45 m.y. of Aegean crust and mantle flow driven by trench retreat. *Geology*, 38(9), 815–818. <https://doi.org/10.1130/G30950.1>
- Carminati, E., Wortel, M. J. R., Spakman, W., & Sabadini, R. 1998. The role of slab detachment processes in the opening of the western-central Mediterranean basins: Some geological and geophysical evidence. *Earth and Planetary Science Letters*, 160(3–4), 651–665. [https://doi.org/10.1016/S0012-821X\(98\)00118-6](https://doi.org/10.1016/S0012-821X(98)00118-6)
- Çenki-Tok, B., Expert, M., Işık, V., Candan, O., Monié, P., & Bruguier, O. 2016. Complete Alpine reworking of the northern Menderes Massif, western Turkey. *International Journal of Earth Sciences*, 105(5), 1507–1524. <https://doi.org/10.1007/s00531-015-1271-2>

- De Boorder, H., Spakman, W., White, S. ., & Wortel, M. J. . 1998. Late Cenozoic mineralization, orogenic collapse and slab detachment in the European Alpine Belt. *Earth and Planetary Science Letters*, 164(3–4), 569–575.
[https://doi.org/10.1016/S0012-821X\(98\)00247-7](https://doi.org/10.1016/S0012-821X(98)00247-7)
- Dercourt, J., Zonenshain, L. P., Ricou, L. E., Kazmin, V. G., Le Pichon, X., Knipper, A. L., ... Biju-Duval, B. 1986. Geological evolution of the Thethis belt from the Atlantic to the Pamirs since the Lias. *Geology*, 123, 241–315.
- Faccenna, C. 2005. Constraints on mantle circulation around the deforming Calabrian slab. *Geophysical Research Letters*, 32(6), L06311. <https://doi.org/10.1029/2004GL021874>
- Faccenna, C., Piromallo, C., Crespo-Blanc, A., Jolivet, L., & Rossetti, F. 2004. Lateral slab deformation and the origin of the western Mediterranean arcs. *Tectonics*, 23(1), n/a-n/a. <https://doi.org/10.1029/2002TC001488>
- Franz, L., & Okrusch, M. 1992. Aragonite-bearing blueschists on Arki island, Dodecanese, Greece. *European Journal of Mineralogy*, 4, 527–537.
- Franz, L., Okrusch, M., Seidel, E., & Kreuzer, H. 2005. Polymetamorphic evolution of pre-Alpidic basement relics in the external Hellenides, Greece. *Neues Jahrbuch Für Mineralogie - Abhandlungen*, 181(2), 147–172. <https://doi.org/10.1127/0077-7757/2005/0013>
- Fytikas, M., Innocenti, F., Manetti, P., Peccerillo, a., Mazzuoli, R., & Villari, L. 1984. Tertiary to Quaternary evolution of volcanism in the Aegean region. *Geological Society, London, Special Publications*, 17(1), 687–699.
<https://doi.org/10.1144/GSL.SP.1984.017.01.55>
- Gautier, P., Brun, J.-P., & Jolivet, L. 1993. Structure and kinematics of Upper Cenozoic extensional detachment on Naxos and Paros (Cyclades Islands, Greece). *Tectonics*, 12(5), 1180–1194. <https://doi.org/10.1029/93TC01131>
- Gessner, K., Piazzolo, S., Güngör, T., Ring, U., Kröner, A., & Passchier, C. W. 2001. Tectonic significance of deformation patterns in granitoid rocks of the Menderes nappes, anatolide belt, Southwest Turkey. *International Journal of Earth Sciences*, 89(4), 766–780. <https://doi.org/10.1007/s005310000106>
- Gessner, K., Gallardo, L. A., Markwitz, V., Ring, U., & Thomson, S. N. 2013. What caused the denudation of the Menderes Massif: Review of crustal evolution, lithosphere structure, and dynamic topography in southwest Turkey. *Gondwana Research*, 24(1), 243–274. <https://doi.org/10.1016/j.gr.2013.01.005>

- Govers, R., & Wortel, M. J. R. 2005. Lithosphere tearing at STEP faults: response to edges of subduction zones. *Earth and Planetary Science Letters*, 236(1–2), 505–523.
<https://doi.org/10.1016/j.epsl.2005.03.022>
- Govers, R., & Fichtner, A. 2016. Signature of slab fragmentation beneath Anatolia from full-waveform tomography. *Earth and Planetary Science Letters*, 450, 10–19.
<https://doi.org/10.1016/j.epsl.2016.06.014>
- Grasemann, B., & Petrakakis, K. 2007. Evolution of the Serifos metamorphic core complex. Inside the Aegean Core Complexes. *Journal of the Virtual Explorer*, Electronic Edition.
- Grasemann, B., Schneider, D. A., Stockli, D. F., & Iglseder, C. 2012. Miocene bivergent crustal extension in the Aegean: Evidence from the western Cyclades (Greece). *Lithosphere*, 4(1), 23–39. <https://doi.org/10.1130/L164.1>
- Grasemann, B., Huet, B., Schneider, D. A., Rice, A. H. N., Lemonnier, N., & Tschegg, C. 2018. Miocene postorogenic extension of the Eocene synorogenic imbricated Hellenic subduction channel: New constraints from Milos (Cyclades, Greece). *GSA Bulletin*.
- Groppo, C., Beltrando, M., & Compagnoni, R. 2009. The P-T path of the ultra-high pressure Lago Di Cignana and adjoining high-pressure meta-ophiolitic units: insights into the evolution of the subducting Tethyan slab. *Journal of Metamorphic Geology*, 27(3), 207–231. <https://doi.org/10.1111/j.1525-1314.2009.00814.x>
- Huet, B., Labrousse, L., & Jolivet, L. 2009. Thrust or detachment? Exhumation processes in the Aegean: Insight from a field study on Ios (Cyclades, Greece). *Tectonics*, 28(3).
- Iglseder, C., Grasemann, B., Schneider, D. A., Petrakakis, K., Miller, C., Klötzli, U. S., ... & Rambahsek, C. 2009. I and S-type plutonism on Serifos (W-Cyclades, Greece). *Tectonophysics*, 473(1), 69–83.
- Jansen, J. B. H. 1973. Geological map of Naxos (1/50 000). *Nation. Inst. Geol. Mining Res.*, Athens.
- Jolivet, L., & Faccenna, C. 2000. Mediterranean extension and the Africa-Eurasia collision. *Tectonics*, 19(6), 1095–1106. <https://doi.org/10.1029/2000TC900018>
- Jolivet, L., & Brun, J. P. 2010. Cenozoic geodynamic evolution of the Aegean. *International Journal of Earth Sciences*, 99(1), 109–138. <https://doi.org/10.1007/s00531-008-0366-4>
- Jolivet, L., Goffé, B., Monié, P., Truffert-Luxey, C., Patriat, M., & Bonneau, M. 1996. Miocene detachment in Crete and exhumation P-T-t paths of high pressure metamorphic rocks, *Tectonics*, 15(6), 1129–1153.
- Jolivet, L., Faccenna, C., Goffé, B., Mattei, M., Rossetti, F., Brunet, C., ... Parra, T. 1998. Midcrustal shear zones in postorogenic extension: Example from the northern Tyrrhenian Sea. *Journal of Geophysical Research: Solid Earth*, 103(B6), 12123–12160. <https://doi.org/10.1029/97JB03616>

- Jolivet, L., Faccenna, C., Goffé, B., Evgenii, B., & Agard, F. 2003. Subduction tectonics and exhumation of high-pressure metamorphic rocks in the Mediterranean orogens. *American Journal of Science*, 303(5), 353–409. <https://doi.org/10.2475/ajs.303.5.353>
- Jolivet, L., Rimmelé, G., Oberhänsli, R., Goffé, B., & Candan, O. 2004. Correlation of syn-orogenic tectonic and metamorphic events in the Cyclades, the Lycian nappes and the Menderes massif. Geodynamic implications. *Bulletin de La Societe Geologique de France*, 175(3), 217–238. <https://doi.org/10.2113/175.3.217>
- Jolivet, L., Faccenna, C., & Piromallo, C. 2009. From mantle to crust: Stretching the Mediterranean. *Earth and Planetary Science Letters*, 285(1–2), 198–209. <https://doi.org/10.1016/j.epsl.2009.06.017>
- Jolivet, L., Lecomte, E., Huet, B., Denèle, Y., Lacombe, O., Labrousse, L., ... Mehl, C. 2010. The North Cycladic Detachment System. *Earth and Planetary Science Letters*, 289(1–2), 87–104. <https://doi.org/10.1016/j.epsl.2009.10.032>
- Jolivet, L., Trotet, F., Monié, P., Vidal, O., Goffé, B., Labrousse, L., Agard, P., & Ghorbal, B. 2010. Along-strike variations of P-T conditions in accretionary wedges and syn-orogenic extension, the HP-LT Phyllite-Quartzite Nappe in Crete and the Peloponnese, *Tectonophysics*, 480, 133-148, doi:110.1016/j.tecto.2009.1010.1002.
- Jolivet, L., Faccenna, C., Huet, B., Labrousse, L., Le Pourhiet, L., Lacombe, O., ... Driussi, O. 2013. Aegean tectonics: Strain localisation, slab tearing and trench retreat. *Tectonophysics*, 597–598, 1–33. <https://doi.org/10.1016/j.tecto.2012.06.011>
- Jolivet, L., Menant, A., Sternai, P., Rabillard, A., Arbaret, L., Augier, R., ... Le Pourhiet, L. 2015. The geological signature of a slab tear below the Aegean. *Tectonophysics*, 659, 166–182. <https://doi.org/10.1016/j.tecto.2015.08.004>
- Katagas, C., & Sapountzis, E. 1977. Petrochemistry of low and medium grade mafic metamorphic rocks from Leros island, Greece. *TMPM Tschermaks Mineralogische Und Petrographische Mitteilungen*, 24(1–2), 39–55. <https://doi.org/10.1007/BF01081744>
- Katagas, C. 1980. Metamorphic zones and physical conditions of metamorphism in Leros Island, Greece. *Contributions to Mineralogy and Petrology*, 73(4), 389-402.
- Laurent, V., Jolivet, L., Roche, V., Augier, R., Scaillet, S., & Cardello, G. L. 2016. Strain localization in a fossilized subduction channel: Insights from the Cycladic Blueschist Unit (Syros, Greece). *Tectonophysics*, 672–673, 150–169. <https://doi.org/10.1016/j.tecto.2016.01.036>.
- Leake, B. E., Woolley, A. R., Arps, C. E., Birch, W. D., Gilbert, M. C., Grice, J. D., ... & Linthout, K. 1997. Report. Nomenclature of amphiboles: report of the subcommittee on

- amphiboles of the international mineralogical association commission on new minerals and mineral names. *Mineralogical magazine*, 61(2), 295-321.
- Lee, J., & Lister, G. S. 1992. Late Miocene ductile extension and detachment faulting, Mykonos, Greece. *Geology*, 20(2), 121-124.
- Lister, G. S., Banga, G., & Feenstra, A. 1984. Metamorphic core complexes of Cordilleran type in the Cyclades, Aegean Sea, Greece. *Geology*, 12(4), 221.
[https://doi.org/10.1130/0091-7613\(1984\)12<221:MCCOCT>2.0.CO;2](https://doi.org/10.1130/0091-7613(1984)12<221:MCCOCT>2.0.CO;2)
- Menant, A., Jolivet, L., & Vrielynck, B. 2016. Kinematic reconstructions and magmatic evolution illuminating crustal and mantle dynamics of the eastern Mediterranean region since the late Cretaceous. *Tectonophysics*, 675, 103–140.
<https://doi.org/10.1016/j.tecto.2016.03.007>
- Oberhänsli, R., Monie, P., Candan, O., Warkus, F., Partzch, J., & Dora, O. 1998. The age of blueschist metamorphism in the Mesozoic cover series of the Menderes Massif. *Schweiz Mineral Petrogr*, 78, 309–316.
- Okrusch, M., & Bröcker, M. 1990. Eclogites associated with high-grade blueschists in the Cyclades archipelago, Greece: A review. *European Journal of Mineralogy*, 2(4), 451–478. <https://doi.org/10.1127/ejm/2/4/0451>
- Parra, T., Vidal, O., & Jolivet, L. 2002. Relation between the intensity of deformation and retrogression in blueschist metapelites of Tinos Island (Greece) evidenced by chlorite–mica local equilibria. *Lithos*, 63(1), 41-66.
- Pasteris, J. D., & Wopenka, B. 1991. Raman spectra of graphite as indicators of degree of metamorphism. *The Canadian Mineralogist*, 29(1), 1-9.
- Pe-Piper, G., & Piper, D. J. W. 2007. Neogene backarc volcanism of the Aegean: New insights into the relationship between magmatism and tectonics. In L. Beccaluva, G. Bianchini, & M. Wilson (Eds.). *Geological Society of America*. Retrieved from [https://doi.org/10.1130/2007.2418\(02\)](https://doi.org/10.1130/2007.2418(02))
- Piomallo, C., & Morelli, A. 2003. P wave tomography of the mantle under the Alpine-Mediterranean area. *Journal of Geophysical Research: Solid Earth*, 108(B2).
<https://doi.org/10.1029/2002JB001757>
- Pourteau, A., Sudo, M., Candan, O., Lanari, P., Vidal, O., & Oberhänsli, R. 2013. Neotethys closure history of Anatolia: Insights from ⁴⁰Ar–³⁹Ar geochronology and P–T estimation in high-pressure metasedimentary rocks. *Journal of Metamorphic Geology*, 31(6), 585–606. <https://doi.org/10.1111/jmg.12034>

- Pourteau, A., Oberhänsli, R., Candan, O., Barrier, E., & Vrielynck, B. 2015. Neotethyan closure history of western Anatolia: a geodynamic discussion. *International Journal of Earth Sciences*, 105(1), 203–224. <https://doi.org/10.1007/s00531-015-1226-7>
- Pourteau, A., Oberhänsli, R., Candan, O., Barrier, E., & Vrielynck, B. 2016. Neotethyan closure history of western Anatolia: a geodynamic discussion. *International Journal of Earth Sciences*, 105(1), 203–224.
- Rabillard, A., Arbaret, L., Jolivet, L., Le Breton, N., Gumiaux, C., Augier, R., & Grasemann, B. 2015. Interactions between plutonism and detachments during metamorphic core complex formation, Serifos Island (Cyclades, Greece). *Tectonics*, 34(6), 1080–1106. <https://doi.org/10.1002/2014TC003650>
- Reinecke, T., Altherr, R., Hartung, B., Hatzipanagiotou, K., Kreuzer, H., Harre, W., ... & Böger, H. 1982. Remnants of a Late Cretaceous high temperature belt on the island of Anafi (Cyclades, Greece). *N. Jb. Miner. Abh*, 145(2), 157–182.
- Rimmelé, G., Jolivet, L., Oberhänsli, R., & Goffé, B. 2003. Deformation history of the high-pressure Lycian Nappes and implications for tectonic evolution of SW Turkey. *Tectonics*, 22(2), 1–21. <https://doi.org/10.1029/2001TC901041>
- Rimmelé, G., Parra, T., Goffé, B., Oberhänsli, R., Jolivet, L., & Candan, O. 2005. Exhumation paths of high-pressure - Low-temperature metamorphic rocks from the Lycian Nappes and the Menderes Massif (SW Turkey): A multi-equilibrium approach. *Journal of Petrology*, 46(3), 641–669. <https://doi.org/10.1093/petrology/egh092>
- Rimmele, G., Oberhansli, R., Candan, O., Goffe, B., & Jolivet, L. 2006. The wide distribution of HP-LT rocks in the Lycian Belt (Western Turkey): implications for accretionary wedge geometry. *Tectonic Development of the Eastern Mediterranean Region*, 260(1), 447–466. <https://doi.org/10.1144/gsl.sp.2006.260.01.18>
- Ring, U., Laws, S., & Bernet, M. 1999. Structural analysis of a complex nappe sequence and late-orogenic basins from the Aegean Island of Samos, Greece. *Journal of Structural Geology*, 21(11), 1575–1601. [https://doi.org/10.1016/S0191-8141\(99\)00108-X](https://doi.org/10.1016/S0191-8141(99)00108-X)
- Ring, U., Glodny, J., Will, T., & Thomson, S. 2010. The Hellenic Subduction System: High-Pressure Metamorphism, Exhumation, Normal Faulting, and Large-Scale Extension. *Annual Review of Earth and Planetary Sciences*, 38(1), 45–76. <https://doi.org/10.1146/annurev.earth.050708.170910>
- Ring, U., Gessner, K., & Thomson, S. 2017. Variations in fault-slip data and cooling history reveal corridor of heterogeneous backarc extension in the eastern Aegean Sea region. *Tectonophysics*, 700, 108–130.

- Roche, V., Laurent, V., Cardello, G. L., Jolivet, L., & Scaillet, S. 2016. Anatomy of the Cycladic Blueschist Unit on Sifnos Island (Cyclades, Greece). *Journal of Geodynamics*, 97, 62–87. <https://doi.org/10.1016/j.jog.2016.03.008>
- Salaün, G., Pedersen, H. A., Paul, A., Farra, V., Karabulut, H., Hatzfeld, D. 2011. High-resolution surface wave tomography beneath the Aegean-Anatolia region: constraints on upper-mantle structure. *Geophysical Journal International*, 190(1), 406–420. <https://doi.org/10.1111/j.1365-246X.2012.05483.x>
- Salaün, G., Pedersen, H. A., Paul, A., Farra, V., Karabulut, H., Hatzfeld, D., ... & SIMBAAD Team. 2012. High-resolution surface wave tomography beneath the Aegean-Anatolia region: constraints on upper-mantle structure. *Geophysical Journal International*, 190(1), 406-420.
- Seidel, E., Kreuzer, H., & Harre, W. 1982. The late Oligocene/early Miocene high pressure in the external Hellenides, *geol. Jb.*, E23, 165-206.
- Spakman, W., & Wortel, R. 2004. A tomographic view on western Mediterranean geodynamics. *The Transmed Atlas-The Mediterranean Region from Crust to Mantle*, 31–52. https://doi.org/10.1007/978-3-642-18919-7_2
- Spakman, W., Wortel, M. J. R., & Vlaar, N. J. 1988. The Hellenic subduction zone: a tomographic image and its geodynamic implications. *Geophysical Research Letters*, 15(1), 60–63.
- Stavropoulos, A., & Gerolymatos, I. 1999. Geological map of Leros, *IGME*.
- Sternai, P., Jolivet, L., Menant, A., & Gerya, T. 2014. Driving the upper plate surface deformation by slab rollback and mantle flow. *Earth and Planetary Science Letters*, 405, 110–118. <https://doi.org/10.1016/j.epsl.2014.08.023>
- Theye, T., Seidel, E., & Vidal, O. 1992. Carpholite, sudoite and chloritoid in low high-pressure metapelites from Crete and the Peloponnese, Greece, *Eur. J. Mineral.*, 4, 487-507.
- Trotet, F., Jolivet, L., & Vidal, O. 2001. Tectono-metamorphic evolution of Syros and Sifnos islands (Cyclades, Greece). *Tectonophysics*, 338(2), 179–206. [https://doi.org/10.1016/S0040-1951\(01\)00138-X](https://doi.org/10.1016/S0040-1951(01)00138-X)
- Urai, J. L., Schuiling, R. D., & Jansen, J. B. H. 1990. Alpine deformation on Naxos (Greece). *Geological Society, London, Special Publications*, 54(1), 509–522. <https://doi.org/10.1144/GSL.SP.1990.054.01.47>
- Van Hinsbergen, D. J. J., Langereis, C. G., & Meulen Kamp, J. E. 2005. Revision of the timing, magnitude and distribution of Neogene rotations in the western Aegean region. *Tectonophysics*, 396(1–2), 1–34. <https://doi.org/10.1016/j.tecto.2004.10.001>

Whitney, D. L., & Evans, B. W. 2010. Abbreviations for names of rock-forming minerals. *American mineralogist*, 95(1), 185-187.

Wopenka, B., & Pasteris, J. D. 1993. Structural characterization of kerogens to granulite-facies graphite: applicability of Raman microprobe spectroscopy. *The American Mineralogist*, 78(5-6), 533-557.

Wortel, M. J. R., & Spakman, W. 2000. Subduction and Slab Detachment in the Mediterranean-Carpathian Region. *Science*, 290(5498), 1910–1917. <https://doi.org/10.1126/science.290.5498.1910>

Wyers, G. P., & Barton, M. 1986. Petrology and evolution of transitional alkaline - sub alkaline lavas from Patmos, Dodecanesos, Greece: evidence for fractional crystallization, magma mixing and assimilation. *Contributions to Mineralogy and Petrology*, 93(3), 297–311. <https://doi.org/10.1007/BF00389389>

Figure captions

Table 1: RSCM results in all units. Indicated are the maximum temperature experienced by the rock and the standard deviation, the number of spectra and the error range (1σ).

Fig. 1. Upper crustal and upper mantle structures of the Eastern Aegean domain and the Western Anatolia. (a) Tectonic map of the Western Mediterranean region showing the main faults and associated kinematic indicators. Data are from this study, and from earlier studies in the Cyclades (see Jolivet *et al.* (2013) and references therein) and in the Menderes Massif and its periphery (Rimmelé *et al.* 2006). Abbreviations: BD (Büyük Menderes detachment); CD (Cretan detachment); D.N (Dilek Nappe); GD (Gediz Menderes detachment); NAF (North Anatolian Fault); NCDS (The North Cycladic detachment system); NPDS (Naxos-Paros Extensional Fault System); Ö.U (Ören unit); SD (Simav Detachment); SMSZ (southern shear zone); TCT (Trans-Cycladic Thrust); WATZ (West Anatolia Transfer Zone); WCDS

(The West Cycladic detachment system). **(b)** Tomographic model of Piromallo & Morelli (2003). The white circle illustrates the schematized position of the slab tearing at ~ 100 km.

Fig. 2. New geological map of Leros Island modified from Stavropoulos and Gerolymatos (1999). Poles of foliation and bedding in both Temenia and Marina units are presented in Schmidt's lower hemisphere equal-area projection. Black lines show the localisation of cross sections.

Fig. 3. Tectonic map of Leros Island with main cross sections. **(a)** Main linear fabrics, foliation trajectories and the main shear zones are indicated. Note that the geometry of the main foliation remains constant across the Marina and Temenia contact. Also indicated is the position of the pictures of Figures 4, 5 and 6. **(b)** Simplified cross sections of Leros. Also indicated are the main results of Raman spectrometry on carbonaceous material. Black and red stars refer to and the main occurrences of index minerals.

Fig. 4. Kinematics of ductile deformation in Temenia unit. **(a)** Detailed view of decametric top-to-the-NE shear bands in metapelites. Note that shear bands are crosscut by a SW-dipping normal fault. **(b)** Asymmetric quartz vein showing a top-to-the-northeast sense of shear. **(c)** Top-to-the-NE asymmetric boudinage of a marble layer within metapelites. **(d)** Metric shear bands in the metapelites and dark marble layers. Note shearing consistently top-to-the-west.

Fig. 5. Large-scale boudinage of the Temenia and Marina units. **(a)** Landscape view of the boudinaged marbles of Temenia. Note that some levels of marble are cross cut by the low-angle contact. **(b)** Landscape view of the boudinaged cover of Marina. Note the local absence

of Permian-Triassic cover and the contact between Temenia unit and the limestones of Marina unit.

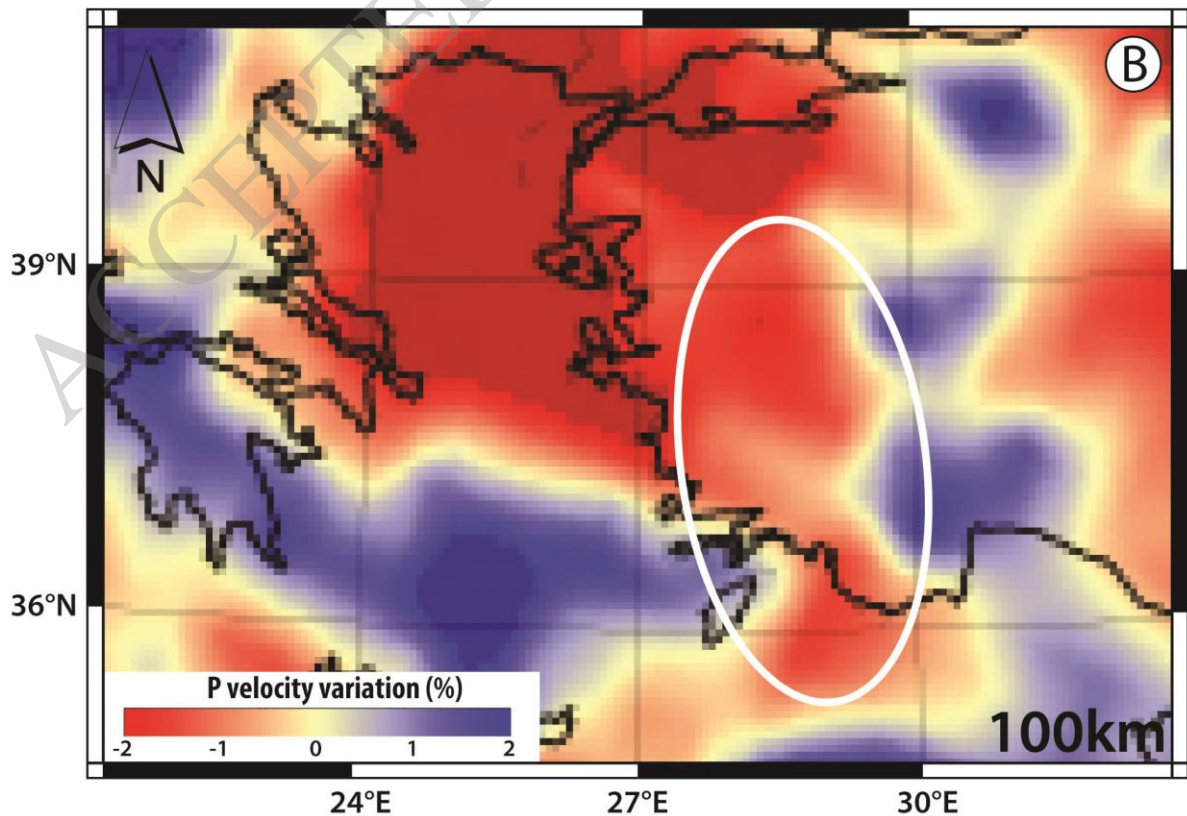
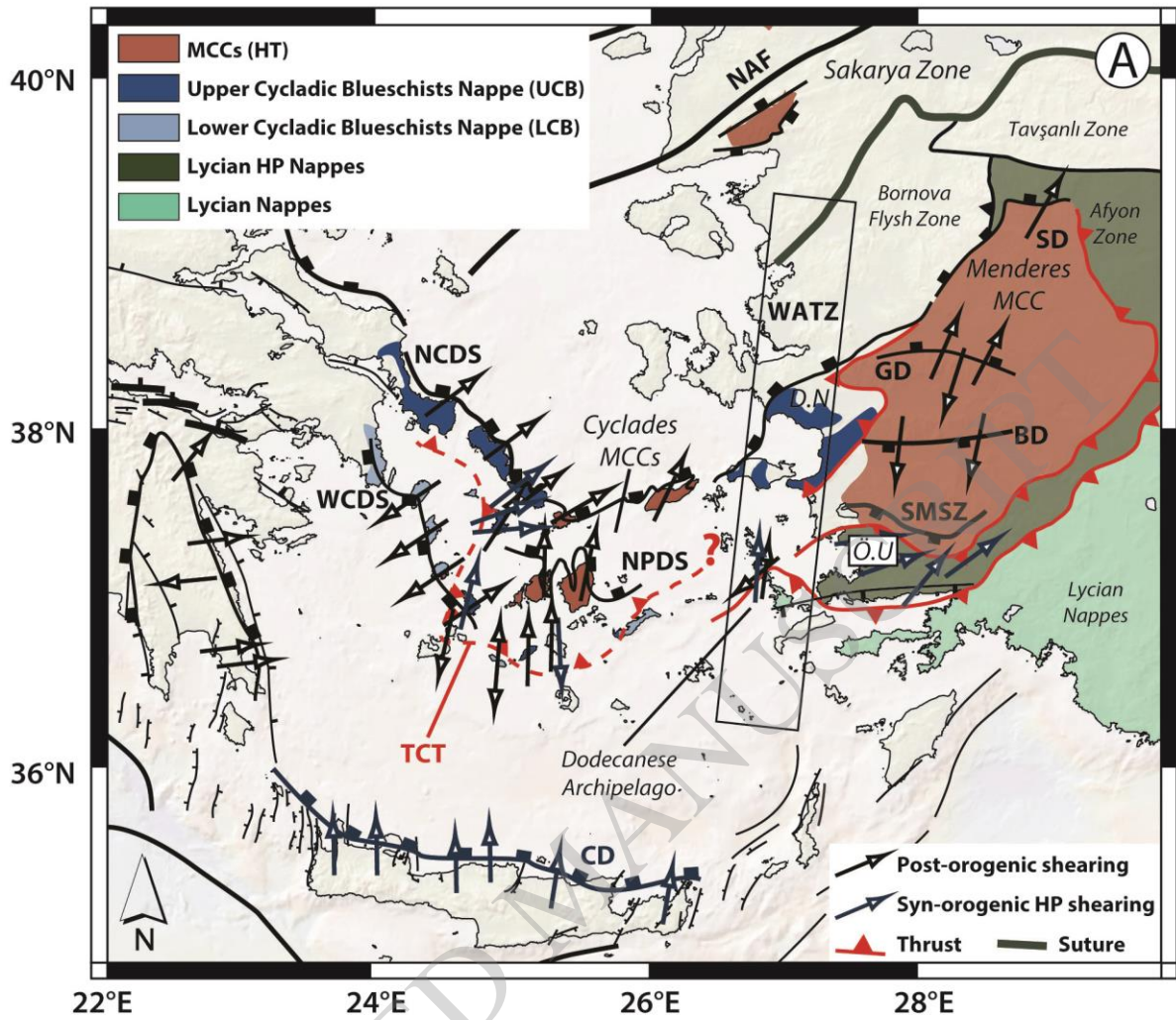
Fig. 6. Kinematic of brittle deformation in both units. (a) Metric low-angle normal faults in the Temenia unit showing top-to-the-west to -southwest deformation. (b) Fault contact between the limestones of Marina and Temenia unit near Xirokampos. Note the thickness of the cataclasites. (c) Large-scale view of the rollover geometry close to Lakki. Poles of bedding in the Neogene sediments are presented in Schmidt's lower hemisphere equal-area projection. (d) Close-up view of the deeper structural level in sediments with a dip value around $\sim 40^\circ$ toward the NE. (e) Main contact between the sediments and the metacarbonate rocks of the Marina unit. (f) Thick breccia within the marbles and associated fault plane with striae. (g) Close-up view of the main low-angle normal fault plane showing two generation of striation.

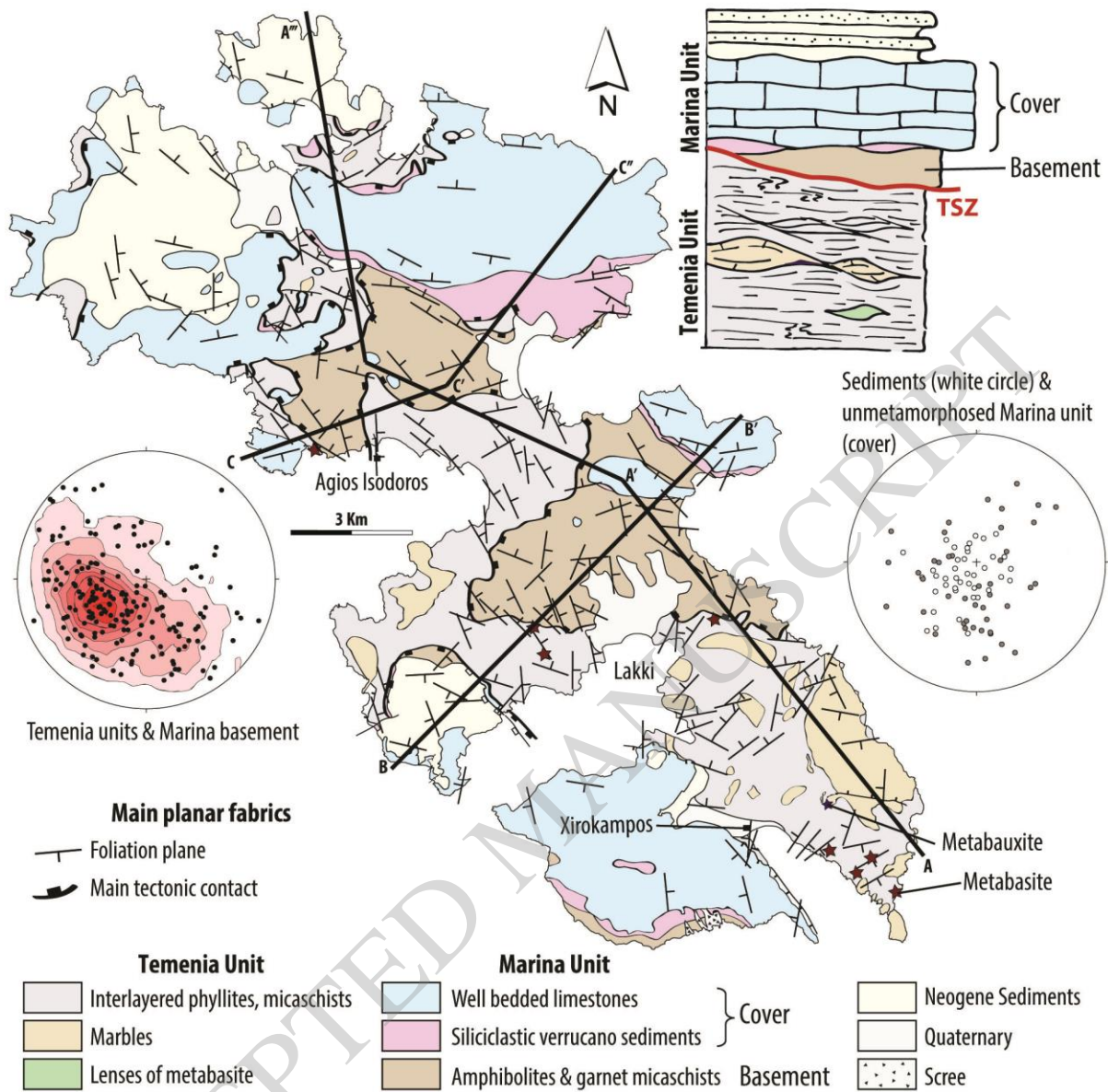
Fig. 7. RSCM distribution and metamorphic record on Leros showing the main metamorphic index minerals. Cam (clinoamphibole); Chl (chlorite); Ep (epidote); Arg (aragonite); Hb (hornblende); Grt (garnet). Abbreviations are from Whitney & Evans (2010).

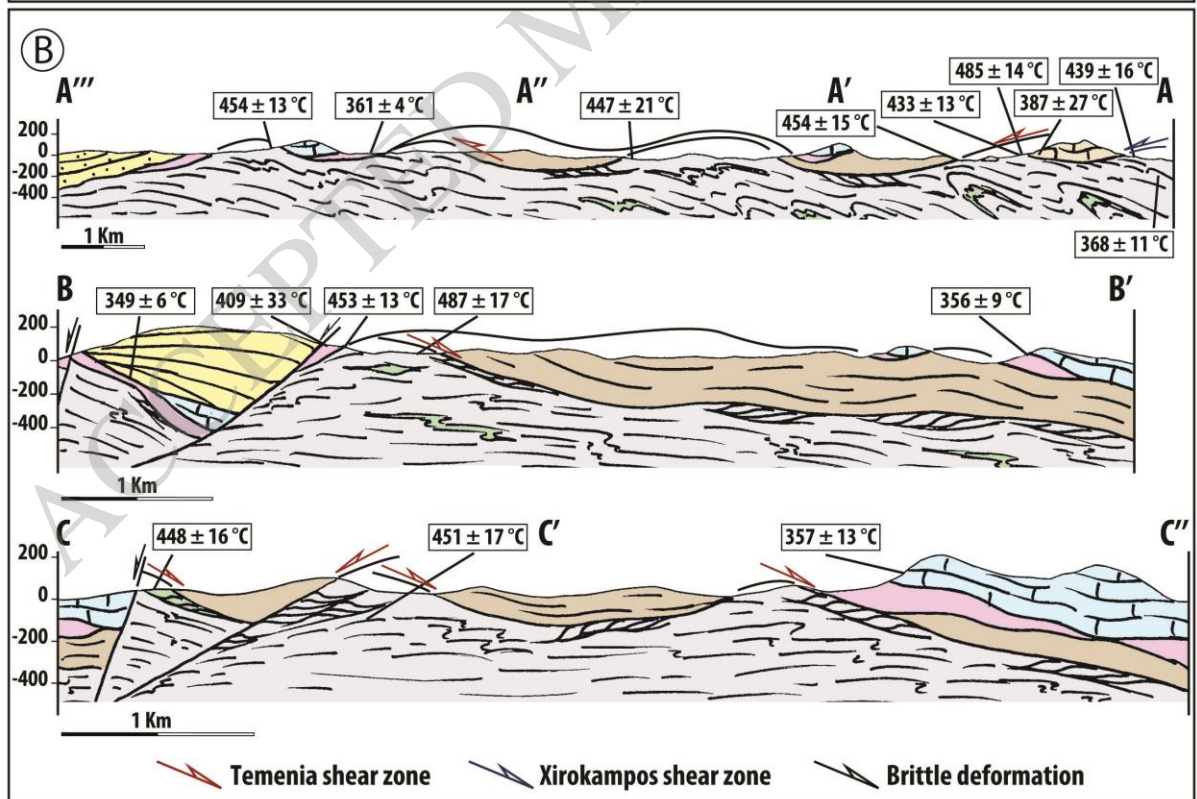
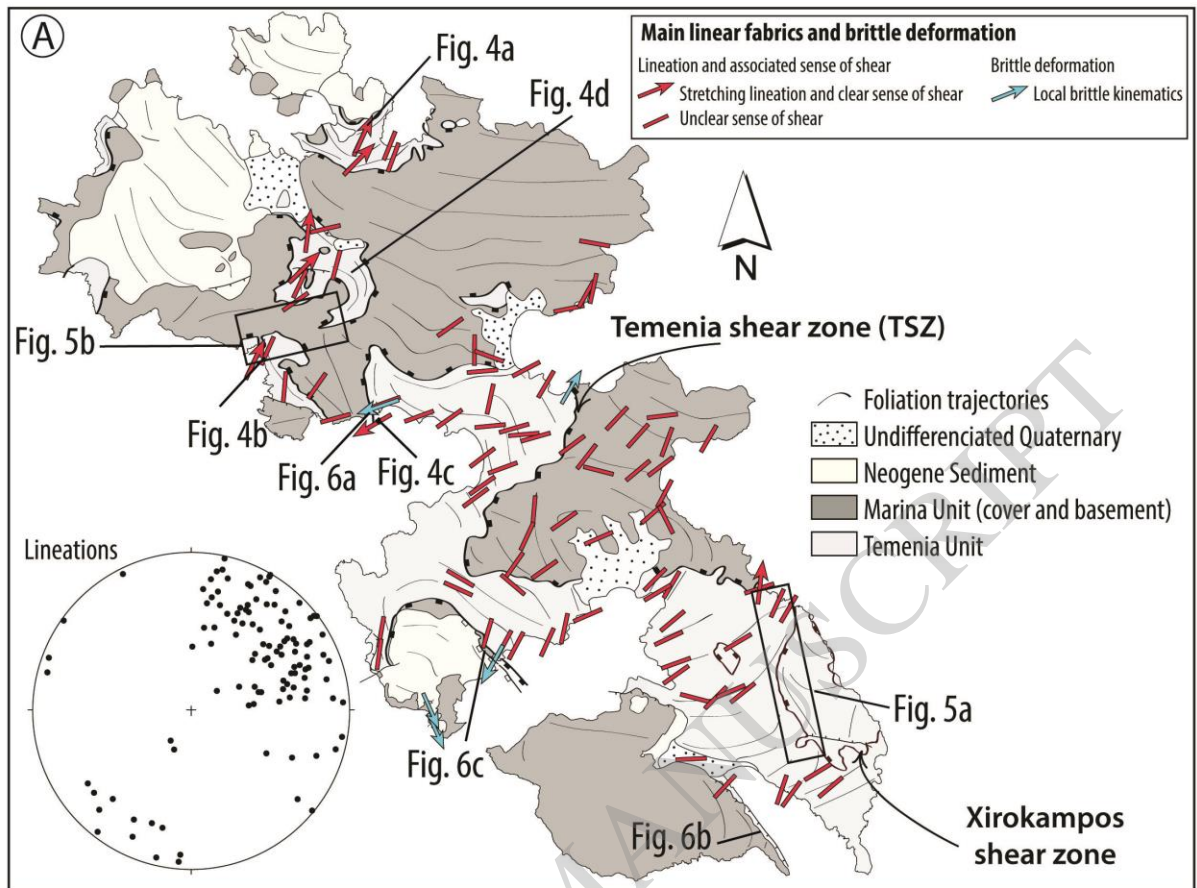
Fig. 8. Metamorphic record on Leros and mineral chemistry. (a) Close up view of garnet bearing micaschist. Mu (muscovite); Q (quartz). (b) Thin section of massive amphibolite. (c) Marble showing locally aragonite occurrence. Cc (calcite); Arg (aragonite). (d) Selection of representative Raman spectra of aragonite. Note the good correlation between the measured spectrum and the reference spectrum. (e) Left picture indicates older-crenulation cleavage defined by blue clinoamphibole and right picture shows retrograde blue clinoamphibole and chlorite within the main foliation plane. Mineral chemistry of metabasites of amphibole

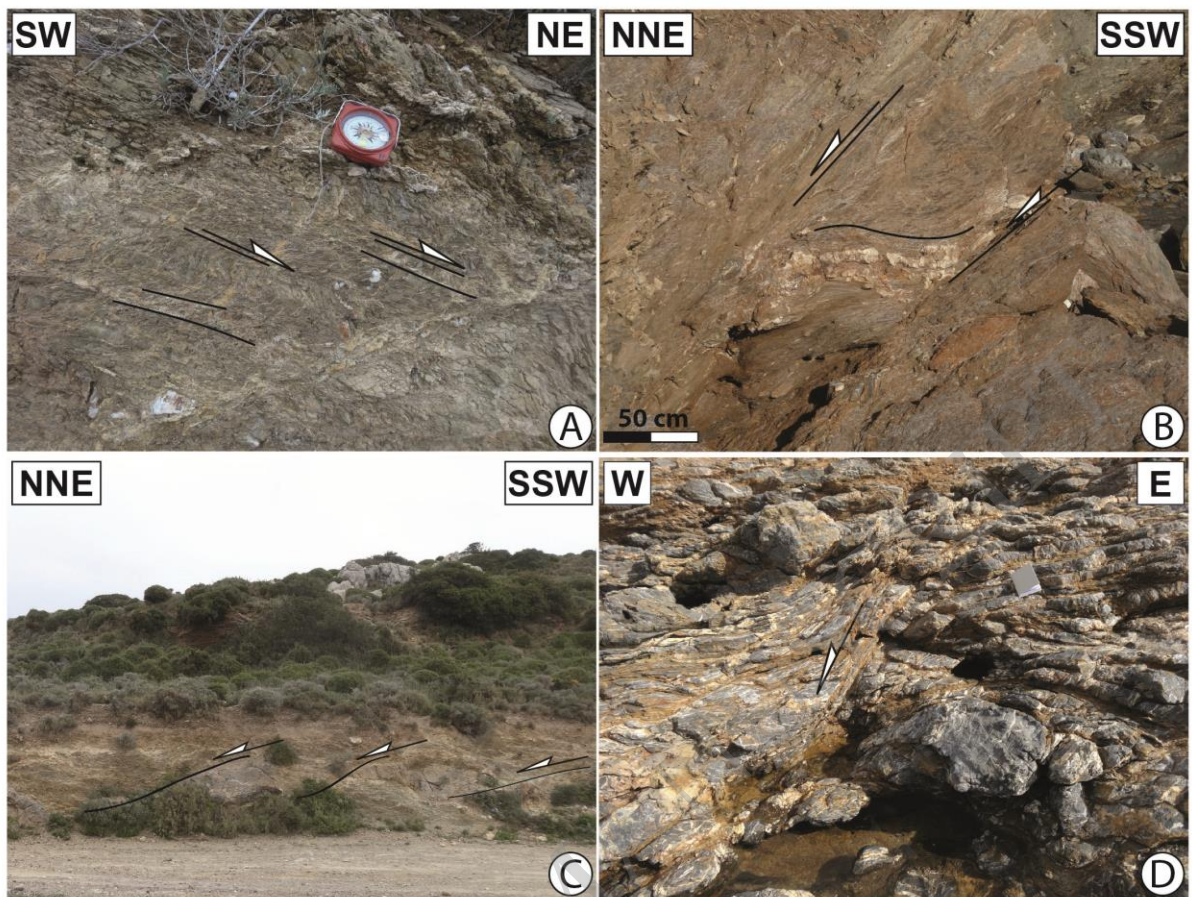
plotted in tetrahedral Si versus Na at the B site. Black spots correspond to the highest values of Na (B site) which are close to the “winchchite-glaucophane” transition (i.e. $\text{Na} > 1.4$). (f) XAl ($\text{Al}/(\text{Fe}^{3+} + \text{Al})$) versus XMg diagrams (after Leake *et al.* 1997). (g) Mineral chemistry of phengite in metabasite.

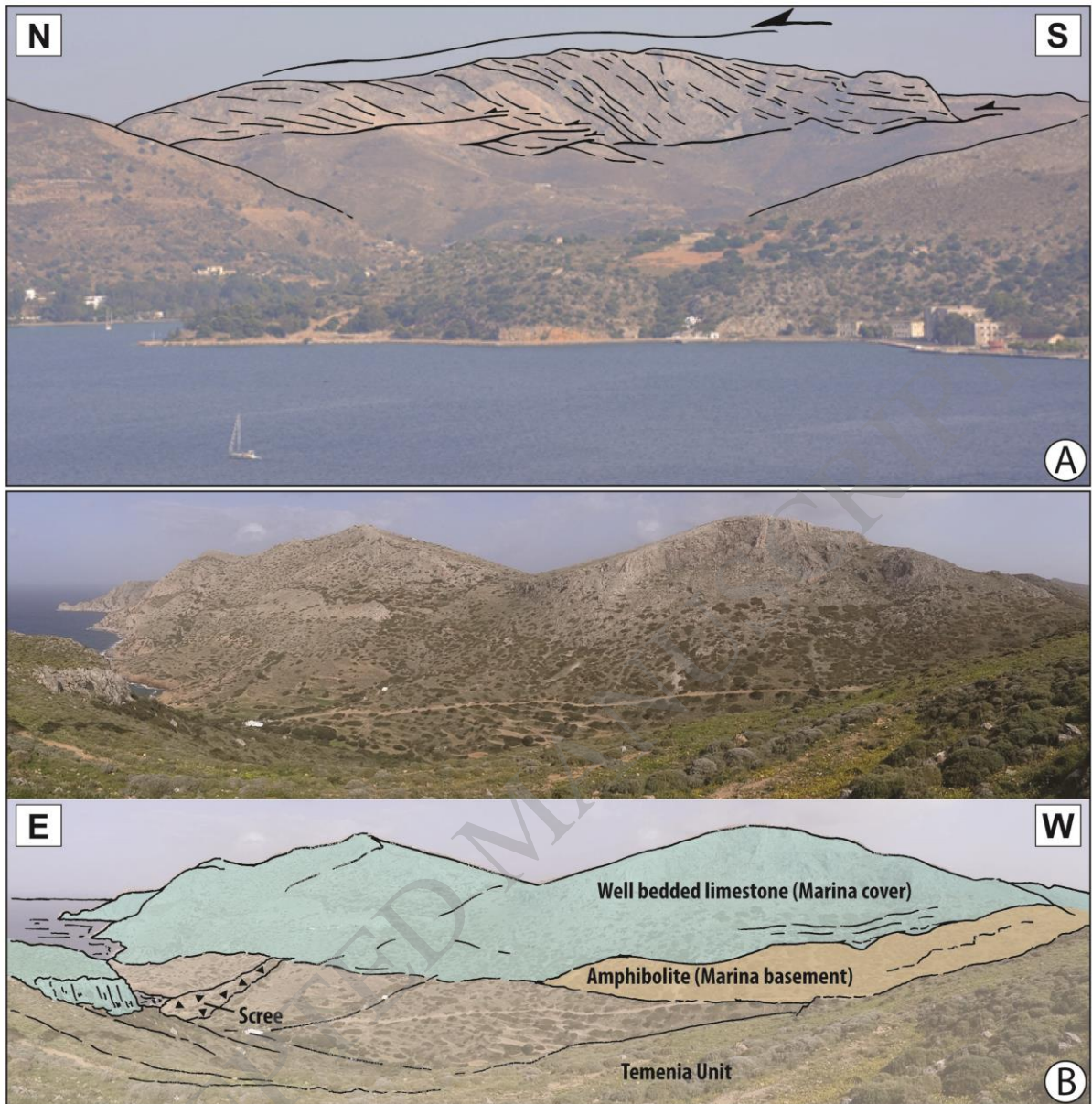
Fig. 9. P-T grid for equilibria in the system NCMASH with activity of $\text{H}_2\text{O} = 0.9$ showing the calculated limiting reactions for the epidote-blueschist facies for the amphibole compositions #5 after Evans (1990). EBS = epidote-blueschist paragenesis, LBS = lawsonite-blueschist paragenesis. GS = greenschist paragenesis. The stability field of the aragonite with T_{max} estimated by the RSCM method. In the same way, we reported the T_{max} conditions of the blue amphibole sample 16-200a. The solid blue line corresponds to the mean value of T_{max} and the dotted line to the errors bars. Mineral abbreviations are indicated in the study of Evan (1990).



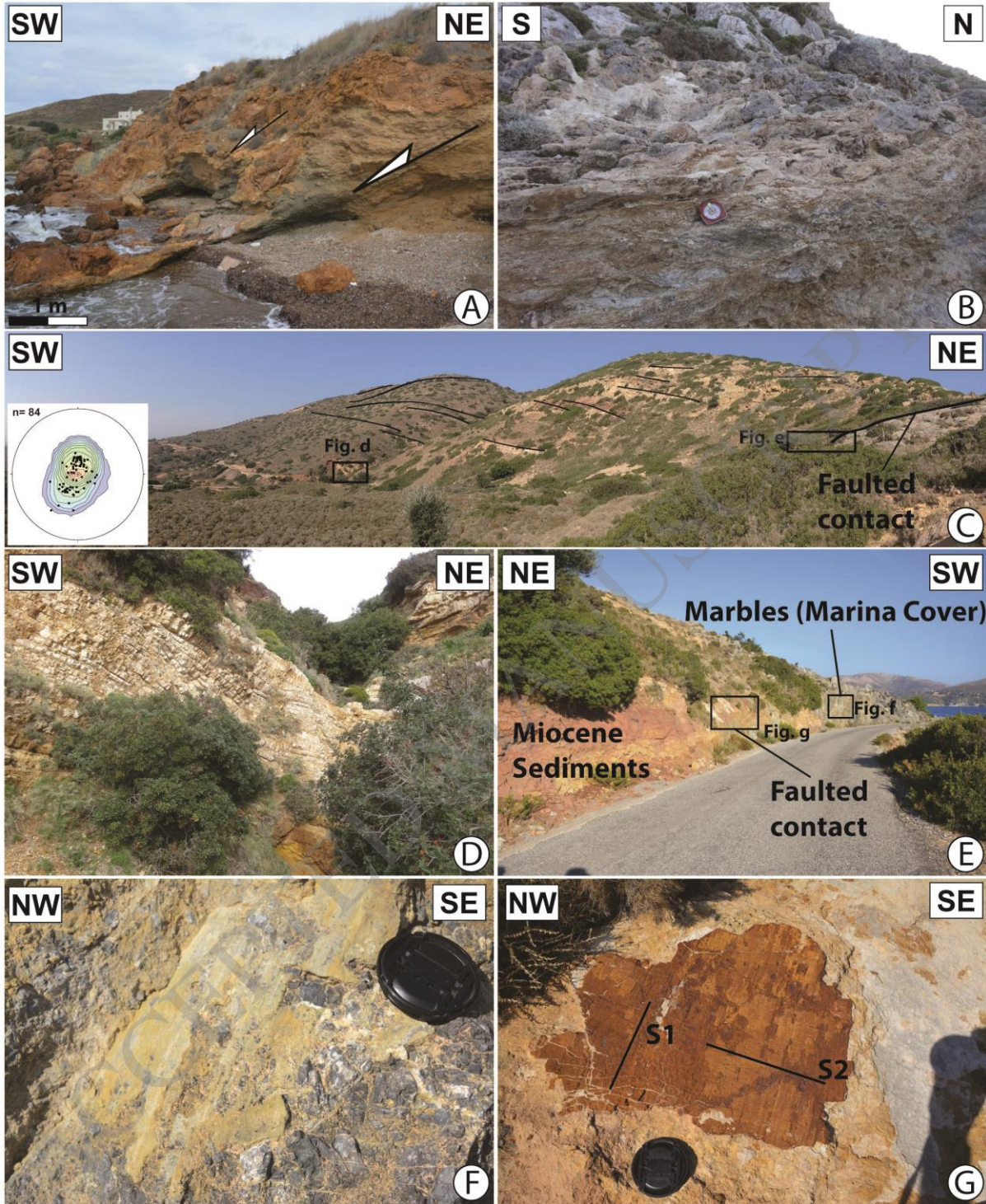


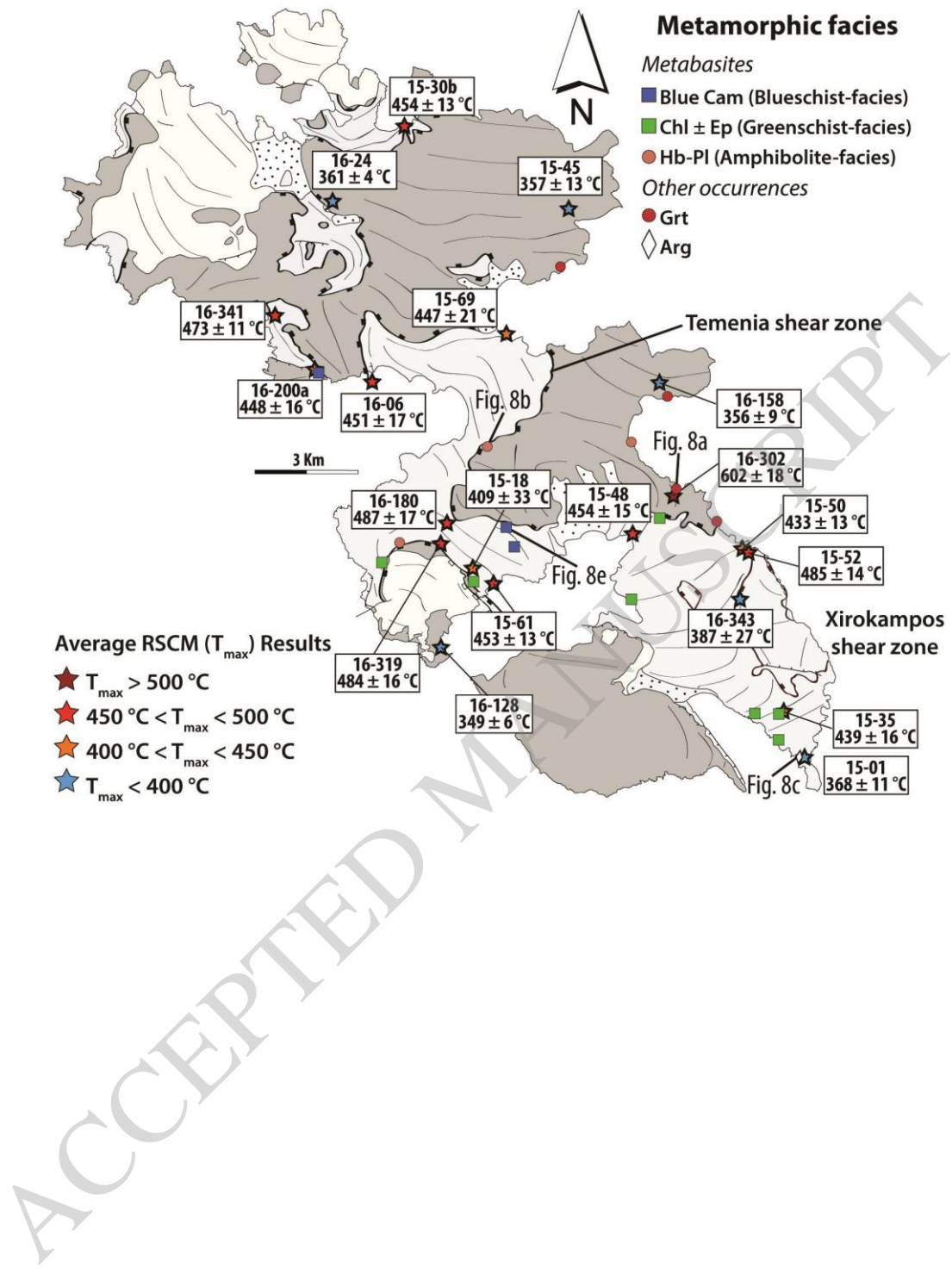


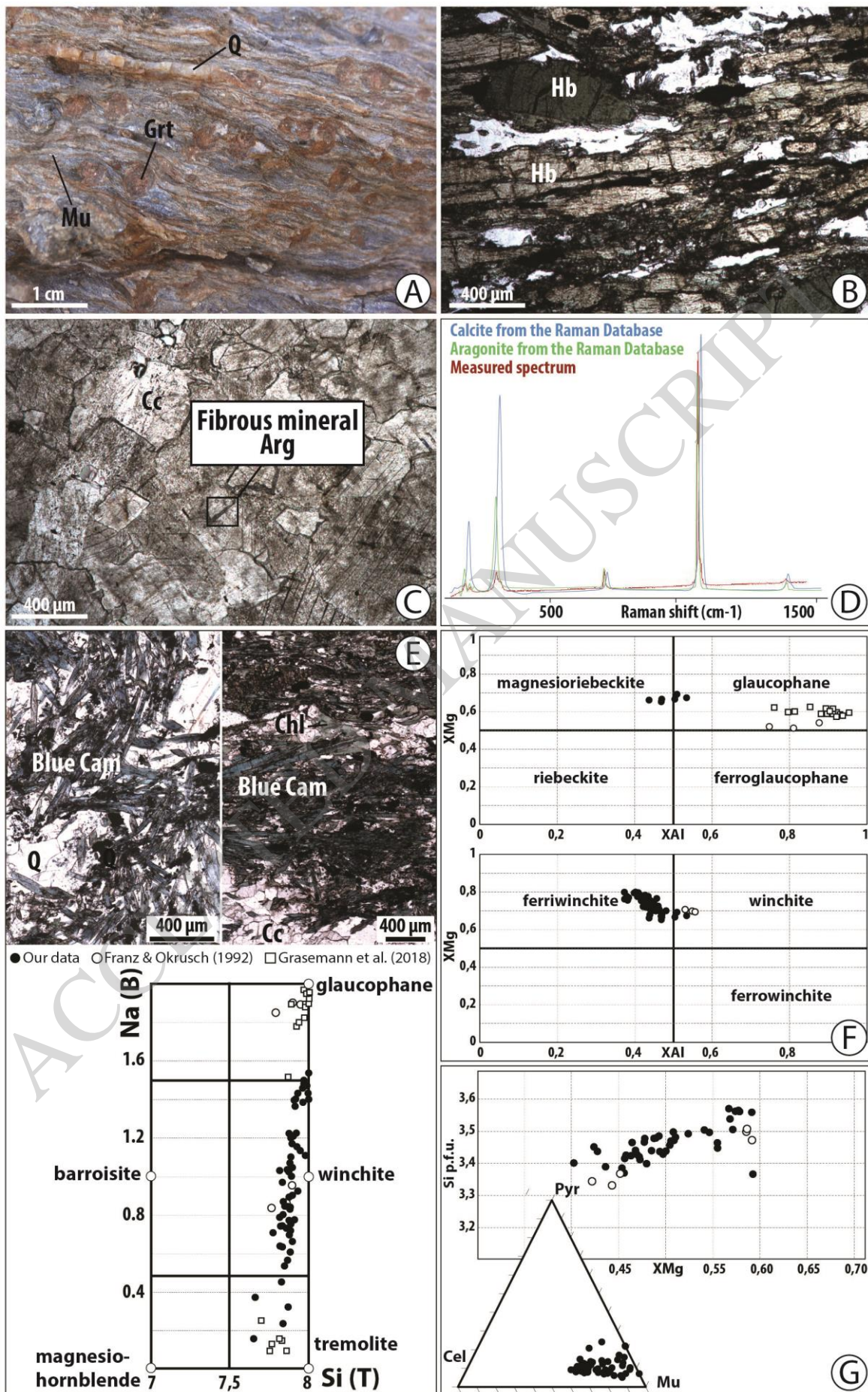


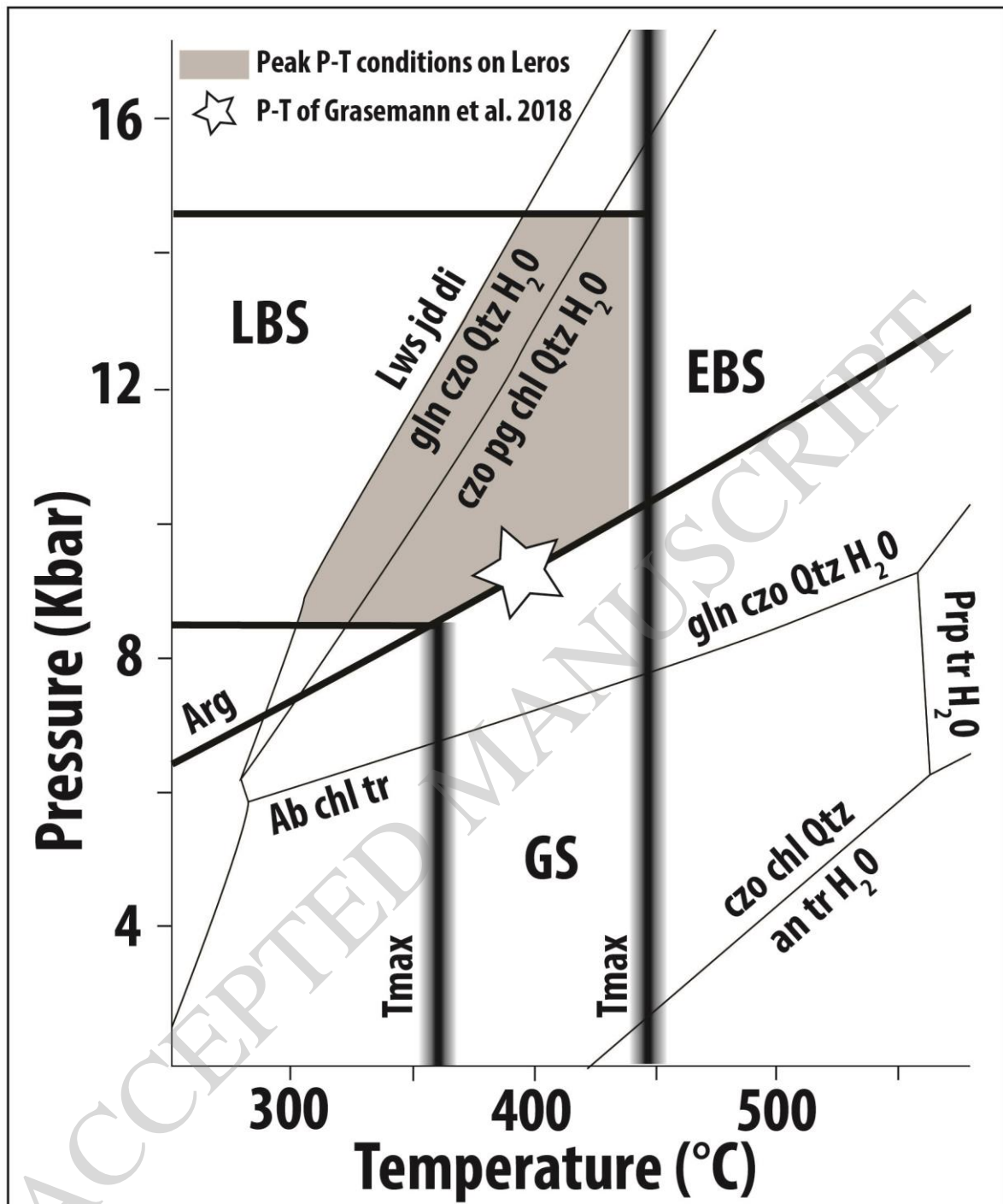


ACCEPTED MANUSCRIPT









Sample	Unit	Lithology	RSCM results			
			Temperature (°C)	Standard Deviation	Spectrum Nb	1 σ
16-128	Marina Cover	Marble	349	6.17	15	1.59
16-158	Marina Cover	Marble	356	8.56	17	2.08
15-45	Marina Cover	Marble	357	13.19	18	3.11
16-24	Marina Cover	Marble	361	4.45	17	1.08
16-343	Marina Cover	Marble	387	26.71	17	6.48
16-302	Marina Basement	Garnet micaschist	602	18.00	13	4.99
15-01	Temenia	Aragonite marble	368	11.00	17	2.67
15-18	Temenia	Dark marble	409	33.14	18	7.81
15-50	Temenia	Micaschist	433	13.25	15	3.42
15-35	Temenia	Micaschist	439	15.74	14	4.21
15-69	Temenia	Dark marble	447	21.47	15	5.54
16-200a	Temenia	Dark marble	448	15.58	16	3.90
16-01	Temenia	Dark marble	451	17.12	15	4.42
15-61	Temenia	Dark marble	453	12.87	14	3.44
15-48	Temenia	Dark marble	454	14.55	17	3.53
15-30b	Temenia	Micaschist	454	12.85	17	3.12
16-341	Temenia	Dark marble	473	11.33	14	3.03
16-319	Temenia	Dark marble	484	15.52	22	3.31
15-52	Temenia	Micaschist	485	13.51	14	3.61
16-180	Temenia	Dark marble	487	16.90	18	3.98

Table 1: RSCM results in all units. Indicated are the maximum temperature experienced by the rock and the standard deviation, the number of spectra and the error range (1σ).